Economic Geology
Vol. 96, 2001, pp. 1827–1853

Miocene and Early Pliocene Epithermal Gold-Silver Deposits in the Northern Great Basin, Western United States: Characteristics, Distribution, and Relationship to Magmatism

DAVID A. JOHN†

U.S. Geological Survey, Mail Stop 901, 345 Middlefield Road, Menlo Park, California 94025

Abstract

Numerous important Miocene and early Pliocene epithermal Au-Ag deposits are present in the northern Great Basin. Most deposits are spatially and temporally related to two magmatic assemblages: bimodal basalt-rhyolite and western andesite. These magmatic assemblages are petrogenetic suites that reflect variations in tectonic environment of magma generation. The bimodal assemblage is a K-rich tholeiitic series formed during continental rifting. Rocks in the bimodal assemblage consist mostly of basalt to andesite and rhyolite compositions that generally contain anhydrous and reduced mineral assemblages (e.g., quartz + fayalite rhyolites). Eruptive forms include mafic lava flows, dikes, cinder and/or spatter cones, shield volcanoes, silicic flows, domes, and ash-flow calderas. Fe-Ti oxide barometry indicates oxygen fugacities between the magnetite-wustite and fayalite-magnetite-quartz oxygen buffers for this magmatic assemblage. The western andesite assemblage is a high K calc-alkaline series that formed a continental-margin arc related to subduction of oceanic crust beneath the western coast of North America. In the northern Great Basin, most of the western andesite assemblage was erupted in the Walker Lane belt, a zone of transtension and strike-slip faulting. The western andesite assemblage consists of stratovolcanoes, dome fields, and subvolcanic plutons, mostly of andesite and dacite composition. Biotite and hornblende phenocrysts are abundant in these rocks. Oxygen fugacities of the western andesite assemblage magmas were between the nickel-nickel oxide and hematite-magnetite buffers, about two to four orders of magnitude greater than magmas of the bimodal assemblage.

Numerous low-sulfidation Au-Ag deposits in the bimodal assemblage include deposits in the Midas (Ken Snyder), Sleeper, DeLamar, Mule Canyon, Buckhorn, National, Hog Ranch, Ivanhoe, and Jarbidge districts; high-sulfidation gold and porphyry copper-gold deposits are absent. Both high- and low-sulfidation gold-silver and porphyry copper-gold deposits are affiliated with the western andesite assemblage and include the Comstock Lode, Tonopah, Goldfield, Aurora, Bodie, Paradise Peak, and Rawhide deposits.

Low-sulfidation Au-Ag deposits in the bimodal assemblage formed under relatively low oxygen and sulfur fugacities and have generally low total base metal (Cu + Pb + Zn) contents, low Ag/Au ratios, and notably high selenide mineral contents compared to temporally equivalent low-sulfidation deposits in the western andesite assemblage. Petrologic studies suggest that these differences may reflect variations in the magmatic-tectonic settings of the associated magmatic assemblages—deposits in the western andesite assemblage formed from oxidized, water-rich, subduction-related calc-alkaline magmas, whereas deposits in the bimodal assemblage were associated with reduced, water-poor tholeiitic magmas derived from the lithospheric mantle during continental extension. The contrasting types and characteristics of epithermal deposits and their affinities with associated igneous rocks suggest that a genetic relationship is present between these Au-Ag deposits and their temporally associated magmatism, although available data do not prove this relationship for most low-sulfidation deposits.

Introduction

MIDDLE to late Tertiary, epithermal Au-Ag deposits in the northern Great Basin (Fig. 1) have been an important source of precious metals for the United States since the discovery of the Comstock Lode in 1859. Production from these deposits through 1996 exceeded 40 million oz (Moz) Au and 555 Moz Ag, mostly from Miocene and younger deposits (Long et al., 1998). Famous districts include Comstock Lode, Tonopah, Goldfield, Aurora, and Bodie, and significant production continues today from large deposits at Round Mountain, Midas, and Rawhide (Fig. 2).

As shown by many workers since Ransome (1907), Lindgren (1933), and Nolan (1933), epithermal gold-silver deposits can be broadly separated into two groups, high-sulfidation (acid-sulfate, quartz-alunite) and low-sulfidation (adularia-sericite) types, based on their ore assemblages and associated hydrothermal alteration (e.g., Heald et al., 1987; White and Hedenquist, 1990; Cooke and Simmons, 2000; Hedenquist et al., 2000). These deposit types reflect distinct variations in fluid composition and the physical environment of ore deposition. High-sulfidation deposits form from relatively oxidized, acidic fluids and low-sulfidation deposits form from reduced, neutral-pH fluids. Whereas a clear genetic relationship is present between magmatism and high-sulfidation deposits (e.g., Rye et al., 1992; Hedenquist and Lowenstern, 1994; Arribas, 1995; Hedenquist et al., 1998), the role of magmas in the formation of low-sulfidation deposits is less obvious, because their hydrothermal systems generally are dominated by meteoric water (O'Neil and Silberman, 1974; Hedenquist and Lowenstern, 1994; Simmons, 1995; Cooke and Simmons, 2000).

John (1999, 2000) and John et al. (1999) showed that low-sulfidation deposits in northern Nevada could be divided into two subtypes based on their ore mineralogy, associated magmatism, and tectonic environment of formation, and they noted that type 1 low-sulfidation deposits contained sulfide

† E-mail: djohn@usgs.gov

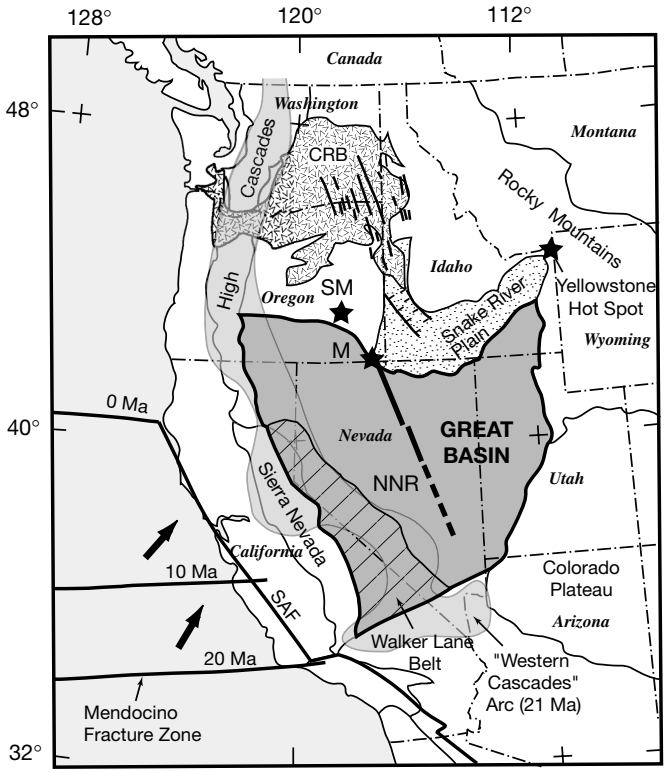

FIG. 1. Index map of the western United States showing middle Miocene igneous and tectonic features. Heavy line indicates the northern Nevada rift. The heavy star at the north end of the rift is the McDermitt caldera (M) and the apparent location of the Yellowstone hot spot at 16.5 Ma. Western graben of the Snake River plain is shown by hachured lines. Columbia River Basalt Group (CRB) shown by vee pattern; feeder dikes in Oregon and Washington indicated by heavy lines. East-west lines along Pacific Coast show approximate location of the Mendocino fracture zone (southern end of the Farallon plate that was being subducted beneath North America) at the different times indicated. Shaded area represents maximum extent of the Miocene continental-margin ("Western Cascades") arc of the western andesite assemblage at about 21 Ma (Christiansen and Yeats, 1992). The arc gradually retreated to the north as the Mendocino fracture zone migrated north shutting off subduction of the Farallon plate and forming the San Andreas fault transform boundary to the southwest (SAF). Modified from Zoback et al. (1994, fig. 1). Walker Lane belt from Stewart (1988). NNR = northern Nevada rift, SM = Steens Mountain.

mineral assemblages transitional between high- and low-sulfidation deposits. Based on deposits in the Great Basin and elsewhere, Hedenquist et al. (2000) suggested that these two subtypes of low-sulfidation deposits should be renamed intermediate-sulfidation and end-member low-sulfidation types to emphasize their mineralogical, magmatic, and tectonic differences.

Most epithermal gold-silver deposits in the northern Great Basin are hosted by middle to late Tertiary igneous rocks (Fig. 2). With the exception of the giant late Oligocene Round Mountain deposit and much smaller deposits in the Atlanta, Fairview, Tuscarora, and Wonder mining districts that are hosted by late Eocene to early Miocene caldera complexes (Fig. 2a; McKee and Moring, 1996), these deposits are associated with two distinct Miocene to Quaternary magmatic assemblages, the western andesite and bimodal basalt-rhyolite assemblages (Fig. 2b and c, Table 1; Christiansen and Yeats, 1992; Ludington et al., 1996b; John et al., 1999). The western andesite assemblage is a subduction-related, continental-margin volcanic arc that formed along the western coast of North America between about 22 to 4 Ma. By contrast, the bimodal basalt-rhyolite assemblage is related to continental rifting (Basin and Range extension) that began about 17 Ma and formed the present physiography of the Great Basin (McKee, 1971; Noble, 1972). Numerous low-sulfidation deposits are present in both magmatic assemblages, whereas high-sulfidation gold-silver deposits are restricted to the western andesite assemblage (John et al., 1999).

This paper is a summary of late Cenozoic magmatism and epithermal gold-silver deposits in the northern Great Basin (north of latitude 37°30'N). The focus is on variations in the composition, tectonic setting, and eruptive style of the Miocene to early Pliocene magmatic assemblages and how these variations may have influenced the types and characteristics of epithermal gold-silver deposits formed in the northern Great Basin. The characteristics of low-sulfidation deposits of the western andesite and bimodal assemblages are compared, and the distinction of intermediate-sulfidation deposits from other low-sulfidation deposits, as proposed by Hedenquist et al. (2000), is discussed. The magmatic relationships and deposit distinctions have important implications for exploration for epithermal deposits in the Great Basin and elsewhere.

Pre-Middle Cenozoic Geologic History of the Northern Great Basin

The northern Great Basin has had a complex and varied geologic history that is part of the evolution of the North American Cordillera (Fig. 3; Burchfiel et al., 1992; Ludington et al., 1996a). In the Late Proterozoic, breakup of the supercontinent Rodinia led to development of a west-facing passive margin at the rifted edge of Precambrian continental crust and a westward-thickening wedge of miogeoclinal sediments on the continental slope and shelf (Stewart, 1980; Karlstrom et al., 1999). The location of the rifted continental margin has been inferred to correspond to the 0.706 isopleth of initial $^{87}Sr/^{86}Sr$ in Mesozoic granitic plutons (Figs. 2 and 3; Kistler, 1991).

The rifted continental margin was the focus of several episodes of contractional and extensional deformation during Paleozoic to early Cenozoic time (Fig. 3). The Late Devonian to Early Mississippian Antler and the Late Permian to Early Triassic Sonoma orogenies thrust eugeoclinal sedimentary rocks of the Roberts Mountains and Golconda allochthons eastward over coeval miogeoclinal rocks of the continental shelf. Mesozoic and early Cenozoic deformation of the Nevadan, Elko, Sevier, and Laramide orogenies was associated with an east-dipping subduction zone beneath western North America, accretion of island-arc terranes, and progressive contraction of the miogeocline from west to east, resulting in younger deformation affecting rocks farther to the east. Extensional deformation has affected the region since the late Eocene (see below).

Subduction-related calc-alkaline magmatism was widespread in the northern Great Basin and most intense in the Middle and Late Jurassic, the Cretaceous, and in the middle Cenozoic (Miller and Barton, 1990; Christiansen and Yeats,

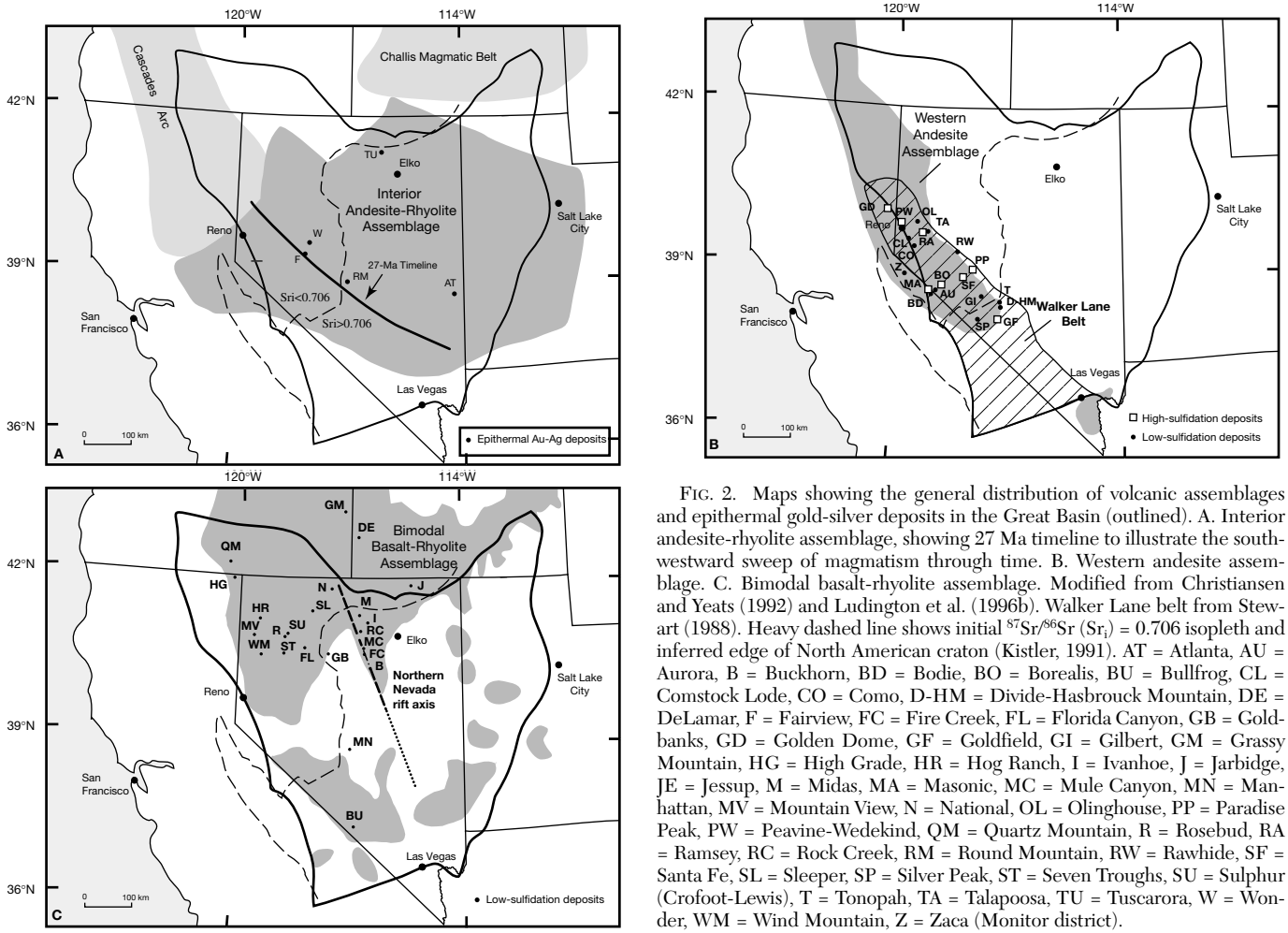

FIG. 2. Maps showing the general distribution of volcanic assemblages and epithermal gold-silver deposits in the Great Basin (outlined). A. Interior andesite-rhyolite assemblage, showing 27 Ma timeline to illustrate the southwestward sweep of magmatism through time. B. Western andesite assemblage. C. Bimodal basalt-rhyolite assemblage. Modified from Christiansen and Yeats (1992) and Ludington et al. (1996b). Walker Lane belt from Stewart (1988). Heavy dashed line shows initial $^{87}Sr/^{86}Sr$ (Sr_i) = 0.706 isopleth and inferred edge of North American craton (Kistler, 1991). AT = Atlanta, AU = Aurora, B = Buckhorn, BD = Bodie, BO = Borealis, BU = Bullfrog, CL = Comstock Lode, CO = Como, D-HM = Divide-Hasbrouck Mountain, DE = DeLamar, F = Fairview, FC = Fire Creek, FL = Florida Canyon, GB = Goldbanks, GD = Golden Dome, GF = Goldfield, GI = Gilbert, GM = Grassy Mountain, HG = High Grade, HR = Hog Ranch, I = Ivanhoe, J = Jarbidge, JE = Jessup, M = Midas, MA = Masonic, MC = Mule Canyon, MN = Manhattan, MV = Mountain View, N = National, OL = Olinghouse, PP = Paradise Peak, PW = Peavine-Wedekind, QM = Quartz Mountain, R = Rosebud, RA = Ramsey, RC = Rock Creek, RM = Round Mountain, RW = Rawhide, SF = Santa Fe, SL = Sleeper, SP = Silver Peak, ST = Seven Troughs, SU = Sulphur (Crofoot-Lewis), T = Tonopah, TA = Talapoosa, TU = Tuscarora, W = Wonder, WM = Wind Mountain, Z = Zaca (Monitor district).

TABLE 1. Comparison of Major Features of the Western Andesite and Bimodal Basalt-Rhyolite Assemblages

Assemblage	Western andesite	Bimodal basalt-rhyolite
Tectonic setting	Subduction-related continental margin arc; erupted mostly within NW-trending Walker Lane belt transtensional zone	Continental rifting: early back-arc extension possibly related to Yellowstone hot spot; later regional continental extension
Compositional characteristics	High K calc-alkaline series	K-rich tholeiitic series; local peralkaline (Na_2O-rich) silicic rocks
Rock compositions	Mostly andesite-dacite, minor rhyolite, rare basalt	Mostly basalt-mafic andesite and rhyolite (subalkaline and peralkaline), minor trachydacite
Volcanic forms	Stratovolcanoes, dome fields, subvolcanic plutons	Mafic lava flows, cinder and/or spatter cones, and sheeted dikes; silicic domes and related pyroclastic rocks; silicic calderas; continental shield volcanoes in western Nevada
Magmatic oxidation state	High (>nickel-nickel oxide (NNO))	Low (<fayalite-magnetite-quartz (FMQ))
Inferred magmatic water content	High (early crystallized hydrous minerals)	Low (hydrous minerals generally absent)
Phenocryst assemblages (intermediate compositions)	Plag + hrnb ± cpx ± opx ± bt + mt + ilm	Plag + cpx ± ol + ilm ± mt
Magmatic sulfides	Uncommon	Pyrrhotite blebs abundant in all compositions

Mineral abbreviations: bt = biotite, cpx = clinopyroxene, hrnb = hornblende, ilm = ilmenite, mt = magnetite, ol = olivine, opx = orthopyroxene, plag = plagioclase

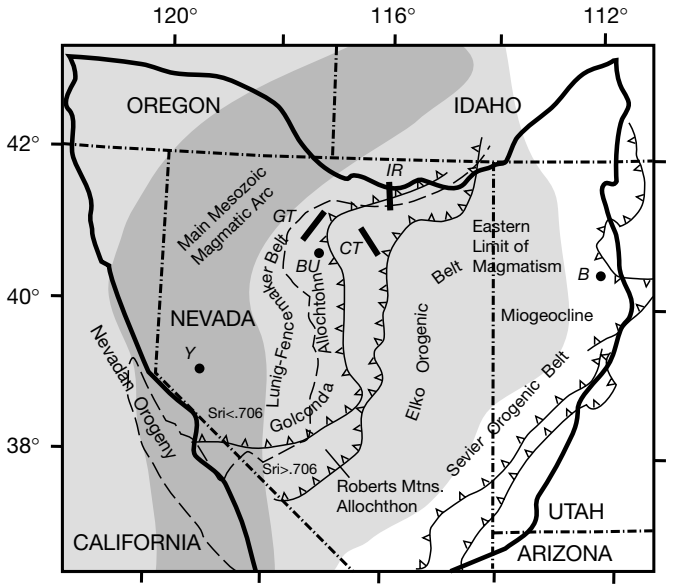

FIG. 3. Map showing generalized distribution of major pre-middle Cenozoic tectonic and magmatic features of the northern Great Basin. Shown are the initial $^{87}Sr/^{86}Sr$ (Sr_i) = 0.706 isopleth and inferred edge of the North America craton (dashed line), eastern limits of the Early Mississippian Roberts Mountains and Permo-Triassic Golconda allochthons, the Jurassic Nevadan, Luning-Fencemaker, and Elko orogenic belts, the Late Cretaceous Sevier orogenic belt, and areas of Mesozoic magmatism (mostly Jurassic and Cretaceous; main magmatic arc (>50% area of all exposed rocks), dark gray; diffuse magmatism (0–50% area of all exposed rocks, light gray). Also shown are major belts (trends) of sedimentary rock-hosted (Carlin-type) gold deposits (CT = Carlin trend, GT = Getchell trend, IR = Independence Range deposits) and other mineral deposits mentioned in text. B = Bingham porphyry copper deposit, Bu = Buckingham porphyry molybdenum deposit, Y = Yerington porphyry copper deposits. Modified from Hofstra and Cline (2000), based on Burchfiel et al. (1992) and Miller and Barton (1990). $^{87}Sr/^{86}Sr$ (Sr_i) = 0.706 isopleth from Kistler (1991).

1992). Many important mineral deposits formed during this time and include porphyry-related Cu, Mo, and Au deposits (e.g., Bingham, Yerington, Buckingham), W skarn deposits, and sedimentary rock-hosted Au deposits, such as the world-class Carlin and Getchell trend deposits (Fig. 3).

Cenozoic Tectonics of the Northern Great Basin

Crustal extension has dominated the Cenozoic tectonic history of the Great Basin. Extension was heterogeneous and occurred during several ages and styles of faulting. Beginning in the late Eocene, rapid, large-magnitude (>100–400%) extension, characterized by multiple sets of closely spaced normal faults, and detachment faults in more deeply exposed terranes, affected much of the Great Basin, but it was irregularly distributed, both in time and space (e.g., Proffett, 1977; Wernicke et al., 1987; Gans et al., 1989; Seedorff, 1991; Axen et al., 1993; Muntean et al., 2001). In general, areas of large-magnitude extension formed first in northeastern Nevada and northwestern Utah and spread south mimicking the southward progression of magmatism (see next section). At about 17 to 16 Ma, more widespread, but smaller magnitude, Basin and Range extension began, producing alternating basins and ranges spaced 20 to 50 km apart that characterize the present physiography of the region. Rapid, large-magnitude extension continued locally after initiation of Basin and Range faulting (e.g., Yerington district; Proffett, 1977; Dilles and Gans, 1995). Mantle-derived basaltic volcanism commonly was associated with Basin and Range faulting, whereas volcanism commonly ceased during periods of rapid, large-magnitude extension (Gans and Bohrson, 1998). Recent estimates of the total amount of Cenozoic extension for the Great Basin generally are 100 to 250 percent (e.g., Seedorff, 1991; Wernicke, 1992; Snow and Wernicke, 2000; Muntean et al., 2001).

The origin(s) of Cenozoic extension in the Great Basin, the relationship of extension to magmatism, and the mechanism of extension in the deep crust and the lithosphere are much debated topics with no general agreement (e.g., Wernicke, 1985, 1992; Gans, 1987; Wernicke et al., 1987; Gans et al., 1989; Axen et al., 1993; Parsons et al., 1994; Gans and Bohrson, 1998; Sonder and Jones, 1999). Spatial and temporal patterns of extension and magmatism in the Great Basin are complex and do not conclusively resolve which models were regionally operative or whether different relationships might apply to different areas and/or different times (e.g., Sonder and Jones, 1999). Regardless of origin, significant extension and crustal thinning of much of the Great Basin occurred prior to Miocene magmatism.

In the Great Basin, intraplate strain between the North America and Pacific plates is broadly partitioned, with extension occurring throughout much of the area and a zone of dextral slip and transtension along its western margin (Walker Lane belt). The dextral slip zone is thought to accommodate much of the relative plate motion that is not taken up along the San Andreas fault, the present plate boundary (Fig. 1; Atwater, 1970; Zoback et al., 1981; Oldow et al., 2001). The Walker Lane belt is a complex northwest-trending zone of diverse topography and strike-slip and normal faulting about 700 km long and 100 to 300 km wide (Figs. 1 and 2; Locke et al., 1940; Stewart, 1988). It contains well-defined Basin and Range block faulting, areas of large-magnitude extension, and strike-slip faults. For example, in the central part of the Walker Lane belt, both strike-slip and normal faulting occurred, possibly in several distinct events, between 22 and 27 Ma, extreme extensional faulting in the Yerington district occurred between 12.5 and 14 Ma, and the present dextral strike-slip faulting began as recently as 7 to 10 Ma (Ekren and Byers, 1984; Stewart, 1988; Hardyman and Oldow, 1991; Oldow, 1992; Dilles and Gans, 1995). Several other areas in the Walker Lane belt have undergone large-magnitude extension in the Miocene and are marked by prominent angular unconformities between late Oligocene to early Miocene ash-flow tuffs and early to late Miocene lava flows and sedimentary rocks (John et al., 1989; Hardyman and Oldow, 1991; Seedorff, 1991; Oldow et al., 1994). Several Miocene epithermal gold-silver deposits in the Walker Lane belt, including Tonopah, Paradise Peak, and Bullfrog, formed during or shortly after large-magnitude extension (John et al., 1989, 1991; Seedorff, 1991; Eng et al., 1996).

Cenozoic Magmatism in the Northern Great Basin

The timing and regional distribution of Cenozoic magmatism in the Great Basin are relatively well known (e.g., McKee et al., 1970; McKee, 1971; Noble, 1972; Stewart and Carlson, 1976; Best et al., 1989; Seedorff, 1991; Christiansen

and Yeats, 1992; McKee and Moring, 1996; Ludington et al., 1996b; John et al., 1999). Recent syntheses of the Cenozoic geology of the United States Cordillera provide a framework that allows division of Cenozoic igneous rocks in the northern Great Basin into three broad tectono-magmatic assemblages: (1) interior andesite-rhyolite (Eocene to early Miocene), (2) western andesite (early Miocene to early Pliocene), and (3) bimodal basalt-rhyolite (middle Miocene to Holocene; Fig. 2).

Interior andesite-rhyolite assemblage

Cenozoic magmatic activity began in the northern Great Basin at about 43 Ma with eruption of silicic ash-flow tuffs and intermediate composition lava flows in northeast Nevada that constitute the early phases of the interior andesite-rhyolite assemblage (Fig. 2a). These rocks are dominantly lava flows that are part of the Tuscarora magmatic belt, a belt of igneous rocks extending southeastward from northeastern California to central Utah that was interior to the continental-margin arc (Figs. 1 and 2a; Stewart and Carlson, 1976; Best et al., 1989; Christiansen and Yeats, 1992; Brooks et al., 1995; McKee and Moring, 1996; Henry and Ressel, 2000). The arc is concave southward and adjoins the slightly older Challis volcanic field in Idaho.

Mid-Cenozoic magmatic activity of the interior andesite-rhyolite assemblage gradually migrated southwestward from northeastern Nevada, forming a succession of arcuate belts that extended nearly continuously east from the Sierra Nevada to the Wasatch Mountains in central Utah. At any one time, magmatism generally was confined to east-west belts about 80 to 150 km wide with generally sharp southern limits, as illustrated by the 27 Ma timeline (Fig. 2a). The youngest rocks in this assemblage were erupted at about 19 Ma and are in the Fairview and Tonopah mining districts along the southwest margin of this assemblage (Fig. 2a and b; Henry, 1996; Ludington et al., 1996b).

Rocks comprising the interior andesite-rhyolite assemblage are mostly dacite to rhyolite ash-flow tuffs and flow-dome complexes with small volumes of andesitic to dacitic lava flows; basaltic rocks are notably rare. Caldera complexes are common, notably in Oligocene to early Miocene rocks in central Nevada and western Utah, where more than 50 calderas have been identified (Best et al., 1989; Ludington et al., 1996b; McKee and Moring, 1996). Plutonic rocks, mostly of granodiorite composition, are exposed locally and include porphyry copper and skarn-related intrusions in the Battle Mountain mining district, Nevada (Theodore and Blake, 1978), and in north-central Utah (e.g., Babcock et al., 1995; Vogel et al., 1998), and porphyry molybdenum-related intrusions at Mount Hope, Nevada (Westra and Riedell, 1996), and Pine Grove, Utah (Keith and Shanks, 1988). Rocks of the interior andesite-rhyolite assemblage are generally calc-alkaline, but they are notably more potassic and silicic than typical arc-related magmas (Christiansen and Yeats, 1992). Most rocks contain hydrous mafic mineral assemblages with abundant hornblende and/or biotite phenocrysts.

Rocks of the interior andesite-rhyolite assemblage generally have been explained as products of subduction-related magmatism related to shallow east-dipping subduction of the Farallon plate beneath western North America in a back-arc setting (Christiansen and Lipman, 1972; Lipman et al., 1972). However, several more recent studies have shown that magmatism had a close spatial and temporal association with crustal extension, and that these magmas were formed by partial mixing of mantle-derived basalt with crustal melts (e.g., Gans et al., 1989; Feeley and Grunder, 1991; Morris et al., 2001, Vogel et al., in press). One model that explains these observations is that removal of the subducted Farallon plate by tearing of the slab near the Canadian and Mexican borders led to upwelling of athenospheric mantle behind the trailing edge of the delaminating lithospheric slab, decompressional melting, and formation of basaltic melts that partially mixed with lower crustal melts (Humphreys, 1995).

Western andesite assemblage

The western andesite assemblage is composed dominantly of lava flows of intermeditate composition, breccias, and hypabyssal intrusions that formed mostly along the northwestern edge of the Great Basin in western Nevada and eastern California (Fig. 2b). This assemblage is part of the continental-margin arc that was active in and west of the modern Cascade Range and extended north into Canada and discontinuously south from southern Nevada into northern Mexico (Figs.1 and 2b; Christiansen and Yeats, 1992; Ludington et al., 1996b; Grose, 2000). The arc formed in response to subduction of oceanic crust beneath the continental margin of North America and was nearly continuous from north to south across the western Great Basin in the early Miocene. The arc gradually retreated northward as the Mendocino fracture zone migrated north, shutting off subduction and forming the San Andreas transform boundary to the south (Fig. 1; Atwater, 1970; Christiansen and Yeats, 1992). In the northern Great Basin, most rocks of this assemblage range in age from about 22 to 4 Ma, and the youngest parts of the assemblage are along the northwestern edge of the Great Basin.

The western andesite assemblage is a high potassium calc-alkaline series (Figs. 4–7; Christiansen and Yeats, 1992; John, 1992; John et al., 1999). Coarsely and abundantly porphyritic hornblende-pyroxene andesite and biotite-hornblende dacite are the most common rock types; small rhyolite intrusions and minor amounts of basalt also are widely distributed.

In western Nevada and northeastern California, most of the western andesite assemblage erupted within the Walker Lane belt (see above; Fig. 2b).

Bimodal basalt-rhyolite assemblage

The bimodal basalt-rhyolite assemblage includes the youngest volcanic rocks in the Great Basin and consists mostly of basalt, basaltic andesite, and rhyolite with relatively scarce rocks with intermediate composition. The bimodal assemblage formed in a continental rifting environment during Basin and Range extension, largely east of the contemporaneous western andesite assemblage (Figs. 2b and c; McKee, 1971; Christiansen and Yeats, 1992; Noble, 1972). The early mafic rocks of the bimodal assemblage include the Steens Mountain Basalt in southeastern Oregon and northwestern Nevada (Figs. 1, 4–7; Carlson and Hart, 1987), and these rocks are temporally and compositionally similar to the Columbia River Basalt in the Columbia plateau (Fig. 1; Hooper and Hawkesworth, 1993).

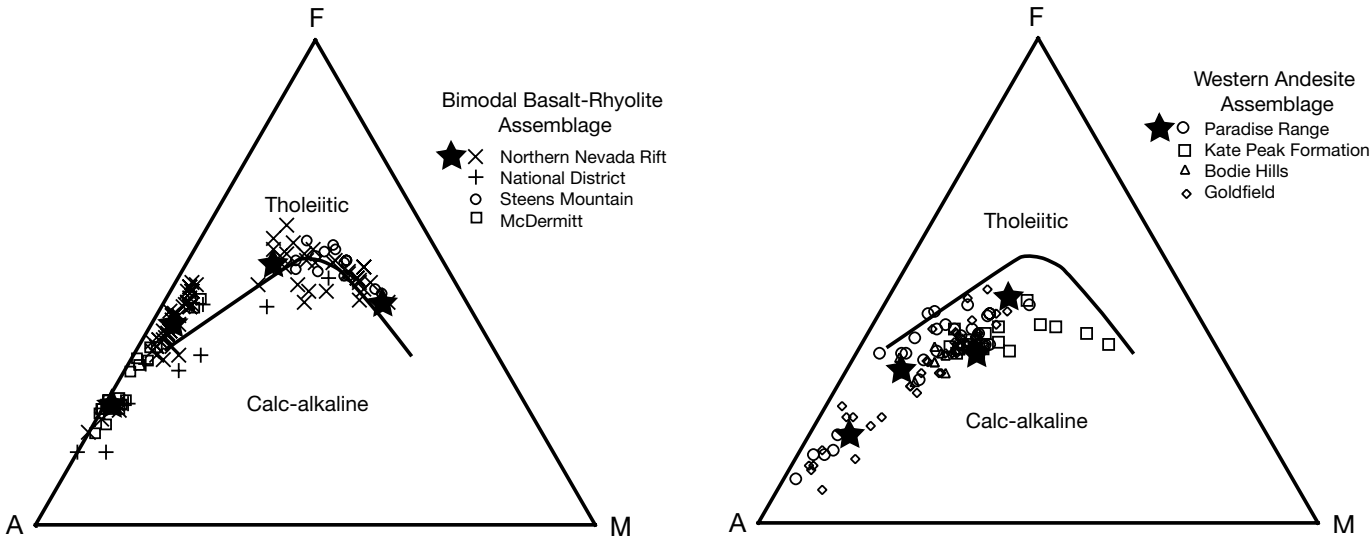

FIG. 4. AFM diagrams for igneous rocks from (A) the bimodal basalt-rhyolite assemblage and (B) the western andesite assemblage. Tholeiitic and calc-alkaline fields from Irvine and Baragar (1971). Data from O'Neil et al. (1973), Whitebread (1976), Conrad (1984), Vikre (1985), Carlson and Hart (1987), John (1992), Wallace and John (1998), John et al. (2000), R.P. Ashley (writ. commun., 2000), and C.D. Henry (writ. commun., 2000).

Volcanism related to the bimodal basalt-rhyolite assemblage began in the northern Great Basin at approximately 16.5 Ma and continues locally to the present day. Bimodal volcanism in the north-central Great Basin began near McDermitt, Nevada, and initially may have been concentrated at the north end of the northern Nevada rift, a narrow north-northwest–trending zone defined by a prominent linear magnetic anomaly (Figs. 1 and 2c; Mabey, 1966; Zoback and Thompson, 1978). The rift, filled in part by mafic dike swarms and lava flows, extends approximately 500 km from the Oregon-Nevada border to south-central Nevada (Blakely and Jachens, 1991; Zoback et al., 1994; John et al., 2000). Most igneous activity related to the rift lasted from about 16.5 to 15 Ma (John et al., 2000).

The bimodal assemblage has a wide range of rock compositions: olivine basalt, pyroxene andesite and basaltic andesite,

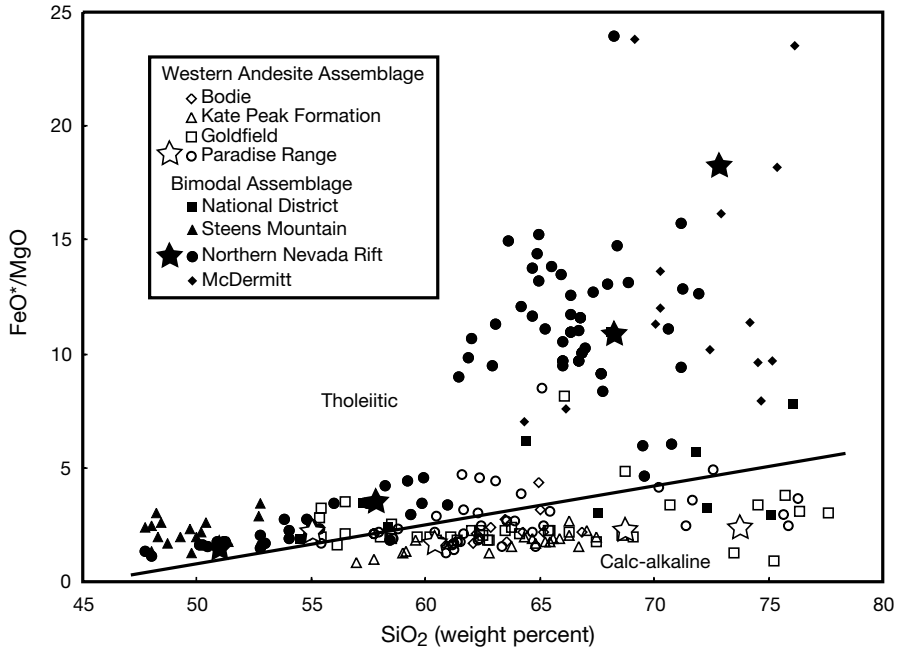

FIG. 5. Silica vs. FeO*/MgO diagram for igneous rocks from western andesite and bimodal basalt-rhyolite assemblages. Tholeiitic and calc-alkaline fields from Miyashiro (1974). Data from Whitebread (1976), Conrad (1984), Vikre (1985), Carlson and Hart (1987), John (1992), Wallace and John (1998), John et al. (2000), R.P. Ashley (writ. commun., 2000), and C.D. Henry (writ. commun., 2000). FeO* = total Fe as FeO.

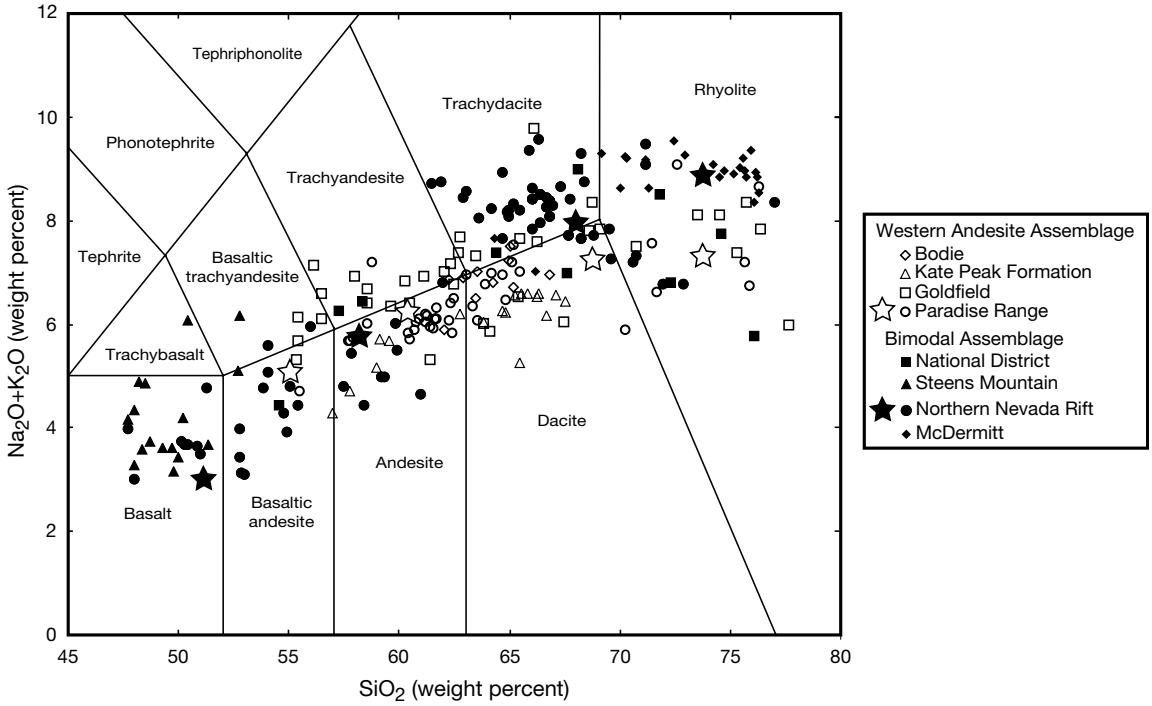

FIG. 6. Total alkali-silica diagram for Miocene igneous rocks from the western andesite and bimodal basalt-rhyolite assemblages. Rock classification from IUGS (Le Bas et al., 1986). Large number of trachydacite samples from the northern Nevada rift are from the northern Shoshone and Sheep Creek Ranges and not representative of the rift as a whole (John et al., 2000). Data from O'Neil et al. (1973), Whitebread (1976), Conrad (1984), Vikre (1985), Carlson and Hart (1987), John (1992), Wallace and John (1998), John et al. (2000), R.P. Ashley (writ. commun., 2000), and C.D. Henry (writ. commun., 2000).

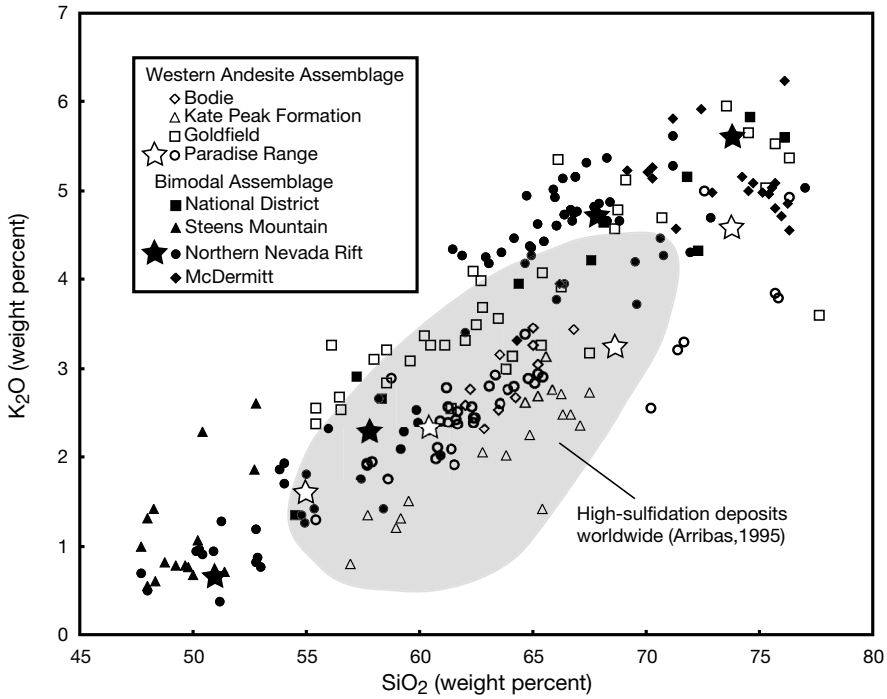

FIG. 7. Silica vs. K_2O diagram for Miocene igneous rocks from the western andesite and bimodal basalt-rhyolite assemblages. Data from O'Neil et al. (1973), Whitebread (1976), Conrad (1984), Vikre (1985), Carlson and Hart (1987), John (1992), Wallace and John (1998), John et al. (2000), R.P. Ashley (writ. commun., 2000), and C.D. Henry (writ. commun., 2000). Note the generally higher K_2O contents for intermediate and silicic compositions of the bimodal assemblage rocks that are mostly outside the range of rocks genetically associated with high-sulfidation gold deposits from throughout the world (Arribas, 1995).

and both subalkaline and peralkaline rhyolite are the most common rock types (Fig. 6). Peralkaline rhyolite ash-flow tuffs (comendites), commonly containing sodic pyroxenes and amphiboles, are a notable part of this assemblage (e.g., McDermitt caldera complex; Conrad, 1984; Rytuba and McKee, 1984). Intermediate compositions (siliceous andesite, dacite, and trachydacite) generally are uncommon except in the central and northern parts of the northern Nevada rift (John et al., 2000). Most rocks of the bimodal assemblage form a potassium-rich tholeiitic series (Figs. 4, 5, and 7; Noble et al., 1988; McKee and Moring, 1996; John et al., 1999). Anhydrous mineral assemblages are typical, suggesting low magmatic water contents (≤3 wt % H_2O; Burnham, 1979; Candela, 1997), and include fayalite-bearing ferrorhyolites that form prominent flow-dome complexes along part of the northern Nevada rift (Wallace, 1993).

The bimodal basalt-rhyolite assemblage was erupted during continental rifting (Basin and Range extension), which formed the modern physiography of the Great Basin (Noble, 1972; Zoback et al., 1981). The older phases of the assemblage were formed in a back-arc environment and were related either to back-arc extension (Christiansen and Lipman, 1972; Carlson and Hart, 1987) and/or to impingement of the Yellowstone hot spot (mantle plume) on the crust at about 16.5 Ma near McDermitt along the Nevada-Oregon border (Fig. 1; Zoback and Thompson, 1978; Christiansen and Yeats, 1992; Pierce and Morgan, 1992; Parsons et al., 1994). The younger parts of the assemblage formed during continental extension unrelated to subduction, possibly due to lithospheric extension over a mantle plume (Noble, 1988; Fitton et al., 1991; Christiansen and Yeats, 1992) or due to a complex combination of processes resulting from the interaction of buoyancy stored in the crust and the removal or alteration of mantle lithosphere (Sonder and Jones, 1999).

Magmatic oxidation state of the western andesite and bimodal basalt-rhyolite assemblages

One of the most striking differences between the bimodal and western andesite assemblages is the variation in phenocryst mineral assemblages and other petrographic features, which suggest that magmas of the western andesite were more oxidized and water rich than magmas of the bimodal assemblage. These inferences are supported by petrologic studies of Fe-Ti oxide minerals in the two assemblages (Fig. 8).

Petrologic studies of the oxidation state of Miocene magmatism in the northern Great Basin are limited. Conrad (1984) studied silicic ash-flow tuffs and related lava flows of the ca. 16 Ma McDermitt caldera complex in north-central Nevada that are part of the bimodal basalt-rhyolite assemblage. He showed that these rocks were erupted at relatively high temperatures and had low oxygen fugacities, between the iron-wustite (IW) and fayalite-magnetite-quartz (FMQ) oxygen buffers (Fig. 8). Honjo et al. (1992) studied Fe-Ti oxide minerals in 12 to 8 Ma rhyolite ash-flow tuffs and lava flows of the Snake River plain north of the Great Basin (Fig. 1). They showed that these rocks were erupted at high temperatures, with most oxygen fugacities near the fayalite-magnetite-quartz oxygen buffer (Fig. 8).

Reconnaissance electron microprobe analyses of Fe-Ti oxide minerals were made on glassy rocks from the bimodal

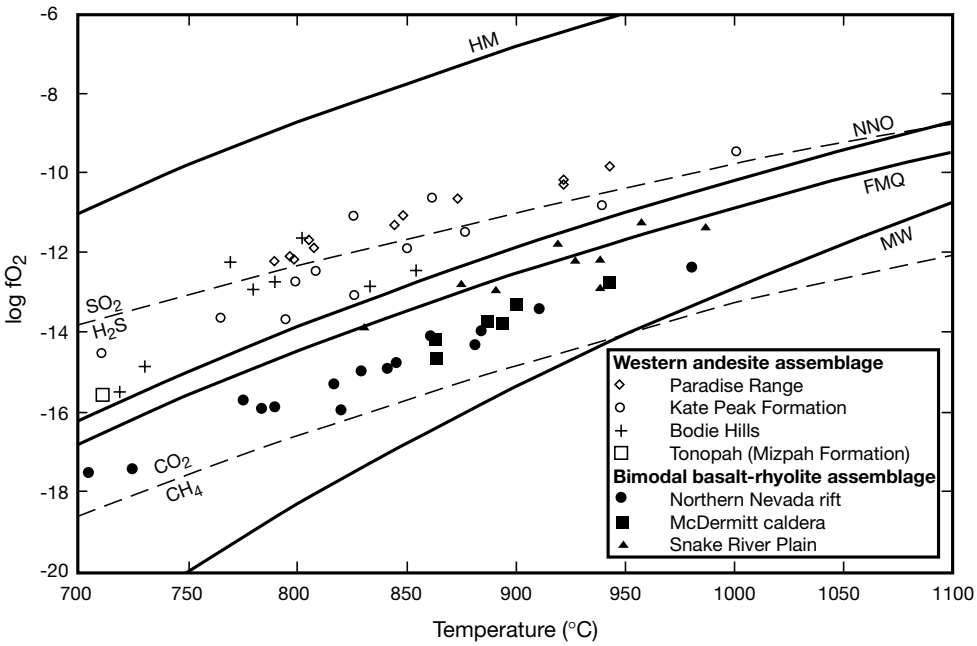

FIG. 8. Temperature-log oxygen fugacity diagram for Miocene igneous rocks of the western andesite and bimodal basalt-rhyolite assemblages. Temperature and oxygen fugacity estimates calculated from electron microprobe analyses of rim compositions of magnetite-ilmenite pairs in glassy lava flows using the computer program QUILF (Andersen et al., 1991). All mineral pairs checked for possible equilibrium using Mg/Mn partitioning relationships (Bacon and Hirschmann, 1988). Data for McDermitt caldera complex from Conrad (1984). Oxygen buffer curves: FMQ = fayalite-magnetite-quartz, HM = hematite-magnetite, MW = magnetite-wustite, NNO, nickel-nickel oxide. SO_2-H_2S and CO_2-CH_4 equilibrium curves from Ohmoto and Goldhaber (1997).

and western andesite assemblages. Samples of 16 to 14.7 Ma rhyolite, dacite, and basalt lava flows and shallow intrusive rocks of the bimodal assemblage collected along the northern Nevada rift (John et al., 2000) yielded temperature and oxygen fugacity estimates similar to Conrad's estimates for rocks from the McDermitt caldera (Fig. 8). These samples include basalts from the northern Shoshone Range that are related temporally and spatially to the Mule Canyon low-sulfidation gold deposit.

In contrast, samples from four volcanic centers in the western andesite assemblage yielded much higher calculated oxygen fugacities, between the nickel-nickel oxide (NNO) and hematite-magnetite (HM) oxygen buffers, about 2 to 4 log units greater than estimates for the bimodal assemblage, and overlapping the SO_2/H_2S buffer curve (Fig. 8). Porphyry copper deposits typically show a similar oxidation state worldwide (Burnham and Ohmoto, 1980). Estimates of magmatic oxygen fugacity for the western andesite assemblage were obtained from 19 to 15 Ma rocks in the southwestern Paradise Range that are related genetically to the Paradise Peak high-sulfidation gold-silver deposit (John et al., 1989, 1991; John, 1992; Sillitoe and Lorson, 1994); from 15 to 8 Ma lava flows and domes in the Bodie Hills that are related temporally and spatially to low-sulfidation deposits in the Bodie and Aurora districts and to a high-sulfidation prospect at East Brawley Peak (O'Neil et al., 1973; Chesterman and Gray, 1975; Osborne, 1991; Breit et al., 1995); from lava flows in the 12 to 11 Ma upper part of the Kate Peak Formation in the Reno-Virginia City area that postdate formation of the Comstock Lode but have similar compositions and phenocryst assemblages to rocks that are spatially and temporally related to the Comstock Lode (Thompson, 1956; Bonham, 1969; Vikre, 1989a; Hudson, 1993; C.D. Henry, writ. commun., 2000); and from the ca. 20.5 Ma Mizpah Formation, which is the major host for low-sulfidation deposits in the Tonopah district (Nolan, 1935; Bonham and Garside, 1979). These data indicate that magmas of the western andesite assemblage were significantly more oxidized than temporally equivalent magmas in the bimodal basalt-rhyolite assemblage.

Comparison of tectonic environments, eruptive products, and compositional variations between magmatic assemblages

Comparison of the temporally equivalent western andesite and bimodal basalt-rhyolite assemblages shows significant differences that reflect variations in the tectonic environment of magma generation and emplacement. These differences include the types of the eruptions, phenocryst assemblages, compositions of the magmas, and duration of magmatic centers (Tables 1–3).

Rocks of the bimodal assemblage tend to occur as (1) widespread, relatively thin mafic lava flows, feeder dikes, and small cinder and/or spatter cones that locally formed continental shield volcanoes; (2) silicic flows and domes with small-volume pyroclastic ejecta; and (3) silicic ash-flow tuffs, commonly of peralkaline composition that locally were related to formation of ash-flow calderas (Fig. 9). Mafic rocks

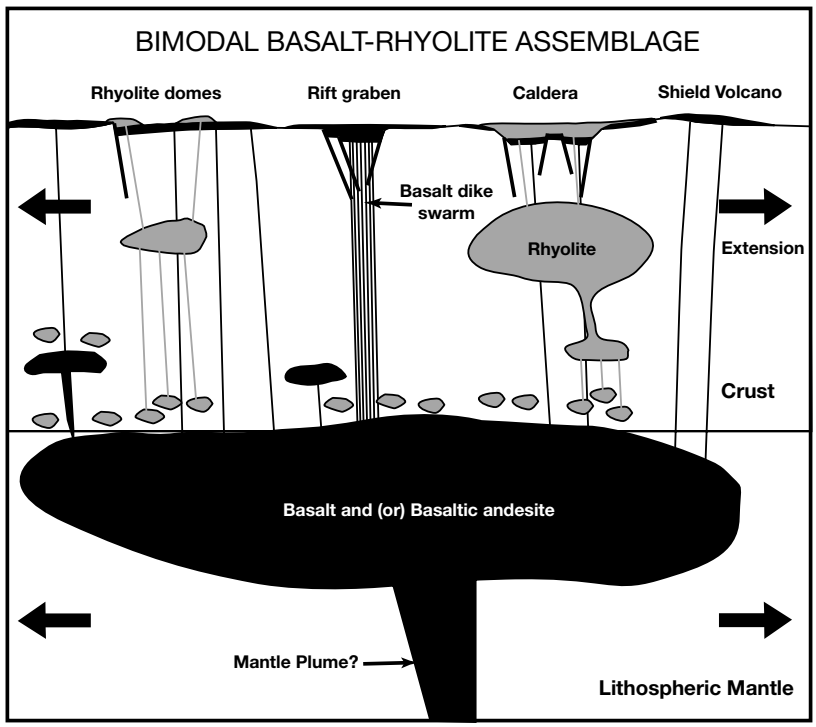

FIG. 9. Cartoon showing magmatic-tectonic setting of the bimodal basalt-rhyolite assemblage in the northern Great Basin. Upwelling of athenospheric mantle into the lithosphere, possibly due to impingement of a mantle plume, led to partial melting of the subduction-modified lithospheric mantle (Fitton at al., 1991). Continental extension allowed rapid ascent of water-poor mafic magmas through the crust and eruption as thin lava flows, shield volcanoes, and dike swarms with little interaction with the crust. Small amounts of partial melting of the base of the crust resulted from basalt underplating and formed reduced, water-poor rhyolitic melts. The rhyolite magmas erupted as domes and lava flows, and local accumulation of these melts in moderate depth magma chambers led to eruptions of ash-flow tuffs and formation of ash-flow calderas.

TABLE 2. Representative Ages of Magmatism and Hydrothermal Ore Deposits in the Western Andesite and Bimodal Basalt-Rhyolite Assemblages, Northern Great Basin

Location	Age range of igneous activity (Ma)	Composition and type of igneous activity	Hydrothermal ore deposits	Type and age (Ma) of hydrothermal ore deposits[1]	Production/reserves	References
Western andesite assemblage						
Southwest Paradise Range/Gabbs Valley Range	23.5(?) to 15.5; mostly 19 to 15.5	Andesite, dacite, and minor rhyolite; lava flows, flow breccias, lahars, domes,and dikes	Paradise Peak	HS, 18.8 to 18.0 (K-Ar)	24,316,000 t ore, 1,626,000 oz Au, >23,991,000 oz Ag	Ekren et al. (1980); Fiannaca (1987); John et al. (1989, 1991); John (1992); Albino and Boyer (1992); Sillitoe and Lorson (1994)
			Goldyke	HS, 18.3 (K-Ar)	Small production	
			Santa Fe, Pearl, Isabella	HS, 19.5 to 19.0 (K-Ar)	12,657,861 t ore, 356,700 oz Au, >721,523 oz Ag	
Virginia Range	20.1 to 10.3	Andesite, dacite, and minor rhyolite; lava flows, flow breccias, lahars, domes and dikes; granodiorite stock	Comstock Lode	LS, 14.1 to 12.2 (K-Ar)	Approx 8.4 Moz Au, approx 193 Moz Ag	Bonham (1969); Vikre et al. (1988); Vikre (1989a, 1998); Albino (1991); Van Nieuwenhuyse (1991); Hudson (1993); John et al. (1999)
			Ramsey-Comstock	LS, 10.5; HS, 9.3 (K-Ar)	Approx 11,000 t ore, 18,650 oz Au	
			Talapoosa	LS, 10.8 (K-Ar); 10.2 (Ar-Ar)	11,215 t ore, 7,549 oz Au, 102,596 oz Ag	
			Gooseberry	LS, 10.3 (K-Ar)	561,317 t ore, 84,866 oz Au, 3,566,143 oz Ag	
			Washington Hill	HS, 12.9 to 10.0 (K-Ar)	No production	
Bodie-Aurora Hills	15.4 to 7.8	Andesite, dacite, and rhyolite; lava flows, flow breccias, lahars, tuff breccia, dikes, and domes	Bodie	LS, 8.0 to 7.1 (K-Ar); 8.41 to 8.23 (Ar-Ar)	1.5 Mt ore, 1,456,000 oz Au, 7,280,000 oz Ag	Silberman et al. (1972); O'Neil et al. (1973); Chesterman and Gray (1975); McKee and Klock (1984); Chesterman et al. (1986); Osborne (1991); Breit et al. (1995); Berger et al. (1999)
			Aurora	LS, 10.3 (K-Ar)	3.86 Mt ore, 1,817,000 oz Au, 20,605,000 0z Ag	
			East Brawley Peak	HS, 13.7 (K-Ar), 12.34 (Ar-Ar)	No production	
			Masonic	HS, 12.8 (K-Ar)	74,694 t ore, 55,791 oz Au, 38,749 oz Ag	
Goldfield	23.4(?) to 20.3	Trachyandesite, rhyodacite, and rhyolite; lava flows and breccias, tuff breccia, and domes	Goldfield	HS, 21.0 to 20.0 (K-Ar)	4.19 Moz Au, 1.45 Moz Ag	Ashley (1974 (1979, 1990); Ashley and Silberman (1976); Vikre (1989b)
Bimodal basalt-rhyolite assemblage						
Snowstorm Mountains	Approx. 15.5 to 13.4	Basalt/basaltic andesite flows and dikes; rhyolite lava flows, dikes, and tuffs	Midas	LS, 15.1-15.2 (Ar-Ar)	322,000 oz Au, 2,123,000 oz Ag (production); 3 Mt ore, 2.45 Moz Au, 29.47 Moz Ag (1999 year end reserves)	Wallace (1993); Goldstrand and Schmidt, 2000); Leavitt et al., 2000b); A.R. Wallace, oral commun. (2000)
Slumbering Hills	>16.5 to 16.3	Rhyolite porphyry; andesite flows and minor tuffs	Sleeper	LS, 16.12 to 15.51 (Ar-Ar)	55.4 Mt ore, 1.68 Moz Au, 2.17 Moz Ag	Nash et al. (1991); Conrad et al. (1993); Nash et al. (1995); Nash and Trudel (1996); Conrad and McKee (1996)
			Jumbo	LS, 17.3 (K-Ar)	Unknown	
Northern Shoshone Range	16.4 to 14.7	Basalt, andesite, and trachydacite; lava flows, dikes, and minor tuffs	Mule Canyon	LS, 15.59 (Ar-Ar)	9 Mt ore, 1 Moz Au (1996 pre-mining reserves)	Thomson et al. (1993); John et al., 2000); John and Wallace, 2000); D.A. John and R.J. Fleck, unpub. data (2000)
Hog Ranch	15.2 to 14.9	Peralkaline rhyolite ash-flow tuff	Hog Ranch	LS, 15.2 to 14.8 (K-Ar)	6,576,000 t ore, 193,000 oz Au, >25,700 oz Ag	Harvey et al. (1986); Bussey (1996) Halsor et al. (1988)
DeLamar	16.6 to 16.1	Basalt, latite, quartz latite, rhyolite; lava flows, domes, and tuff breccia	DeLamar	LS, 15.7 (K-Ar)	19,582,000 t ore, 943,589 oz Au, 37,936,000 oz Ag	

[1] HS = high-sulfidation, LS = low-sulfidation

TABLE 3. Representative Chemical Analyses of the Bimodal Basalt-Rhyolite and Western Andesite Assemblages

	Bimodal basalt-rhyolite assemblage				Western andesite assemblage			
Sample no.	1	2	3	4	5	6	7	8
Field no.	99-DJ-5	99-DJ-21	97-DJ-3	97-DJ-7	84-DJ-232	99-PR-8	99-PR-4	84-DJ-113
SiO_2 (wt %)	50.81	58.02	68.28	73.84	55.18	60.38	68.71	73.78
Al_2O_3	16.72	14.16	13.54	13.10	19.07	16.98	16.19	14.34
FeO*	9.14	9.91	6.01	2.81	7.29	4.91	2.63	1.74
MgO	7.99	3.00	0.54	0.14	3.35	2.97	1.19	0.72
CaO	10.70	6.42	2.58	0.84	7.89	7.46	3.38	1.57
K_2O	0.53	2.34	4.70	5.55	1.58	2.30	3.25	2.76
Na_2O	2.58	3.42	3.27	3.29	3.51	3.93	3.97	4.57
TiO_2	1.09	1.76	0.76	0.30	1.12	0.67	0.42	0.26
P_2O_5	0.28	0.78	0.23	0.11	0.50	0.31	0.18	0.11
MnO	0.16	0.18	0.08	0.03	0.10	0.09	0.08	<.03
Ba (ppm)	342	888	1,614	1,161	1,050	1,269	1,174	1,000
Rb	8	60	150	206	34	54	89	140
Sr	282	346	240	109	1,220	910	694	230
Zr	88	204	380	347	110	133	148	126
Y	27	42	50	83	na	18	13	10
Nb	5.9	14.1	24.8	32.9	<10	5.5	9	10
La	12.5	36.5	64.8	97.1	28.0	22.4	28.0	52
Ce	26.5	73.6	121.6	185.7	57.5	41.7	49.6	46
Ta	0.29	0.86	1.46	2.40	0.44	0.39	0.78	na
Th	2	7	18	27	3.9	3	9	na
Mg#	60.9	35.1	13.7	8.2	45.0	51.9	44.6	42.4
Ba/La	27	24	25	12	38	57	42	19
K/La	353	531	602	474	469	855	964	730
Ba/Nb	58	63	65	35	>105	231	130	100
Zr/Nb	15	14	15	11	>11	24	16	13
Ba/Ta	1,170	1,033	1,106	483	2,386	3,269	1,507	

Notes: Major and trace element analyses by XRF techniques; REE, Ta, and Th by ICP-MS (samples 1-4, 6-7) or INAA (sample 5); analyses 1-4 and 6-7 performed at GeoAnalytical Laboratory, Washington State University; analyses 5 and 8 by USGS laboratories, Denver, CO

Major elements recalculated to 100% volatile free; FeO* = total Fe as FeO; na = not analyzed; Mg# =100*MgO/(MgO + FeO*) (mole percent)

Sample descriptions: 1 = partly glassy, coarsely porphyritic olivine-plagioclase-clinopyroxene basalt flow, base of Mule Canyon sequence, northern Shoshone Range, NV; 2 = devitrified aphyric andesite flow, top of Mule Canyon sequence, northern Shoshone Range, NV; 3 = glassy, porphyritic plagioclase-clinopyroxene-olivine dacite, southwestern Sheep Creek Range, NV; 4 = devitrified, coarse-grained sanidine-quartz-plagioclase-olivine rhyolite porphyry dome, southwest Sheep Creek Range, NV; 5 = devitrified, vesicular fine-grained olivine-bearing basaltic andesite lava flow, Paradise Range, NV; 6 = glassy, medium-grained hornblende-plagioclase-clinopyroxene andesite, southwestern Paradise Range, NV; 7 = glassy, fine-grained biotite-hornblende-plagioclase dacite, southwestern Paradise Range, NV; 8 = devitrified, medium-grained biotite-quartz-sanidine-plagioclase rhyolite dike, southwestern Paradise Range, NV

and rocks of intermediate composition generally have only sparse phenocrysts of plagioclase, olivine, clinopyroxene, and Fe-Ti oxides. Silicic rocks commonly contain quartz and Fe-rich olivine phenocrysts. Phenocrysts of hydrous minerals (biotite and/or hornblende) are absent in most rocks, even those with potassium-rich, intermediate to silicic compositions (John et al., 1999, 2000), suggesting low magmatic water contents (≤3 wt %; Burnham, 1979; Candela, 1997). Ilmenite forms prominent phenocrysts in all compositions, whereas titanomagnetite is sparse or absent, particularly in rocks of intermediate and silicic compositions. Magmatic sulfides (mostly pyrrhotite) are common in all compositions. These characteristics and magmatic temperature and oxygen fugacity estimates discussed above indicate that magmas of the bimodal assemblage were relatively high temperature, water poor, and had low oxygen fugacities and low viscosities, as previously noted along the Snake River plain by Honjo et al. (1992).

Rocks of the western andesite assemblage generally formed stratovolcanoes, dome fields, and subvolcanic intrusions, including granitoid plutons. Lahars and flow breccias are common. Most rocks are strongly porphyritic, and they contain abundant phenocrysts of hydrous minerals (hornblende ± biotite), as well as plagioclase, clino- and orthopyroxenes, and Fe-Ti oxide minerals, suggesting high magmatic water contents. Titanomagnetite is a prominent phenocryst phase in all rock compositions, whereas ilmenite is sparse to absent. These characteristics and Fe-Ti oxide data discussed above indicate that the western andesite magmas were water rich (>3–5 wt % H_2O) and had relatively high oxygen fugacities (Carmichael, 1967; Burnham, 1979; Luhr, 1992; Candela, 1997).

Models linking stress regime, rate of magma supply, and volcanism are consistent with the observed types of eruptions and with the variable stress regimes inferred for the western andesite and bimodal assemblages in the northern Great Basin (Nakamura, 1977; Hildreth, 1981; Takada, 1994; Tosdal and Richards, 2001). Much of the western andesite assemblage was erupted during oblique subduction along the western coast of North America in the Walker Lane belt, a region of transcurrent faulting containing local transtensional zones that may have focused magma emplacement (e.g., Breit et al., 1995; Berger and Drew, 1997; Berger et al., 1999). In this tectonic environment, moderate to high rates of magma supply

coupled with low differential horizontal stress allowed volatile-rich magmas to rise along dilatant zones to shallow crustal levels through buoyancy rather than from magmatic overpressuring (Fig. 10). This resulted in formation of subcircular polygenetic stratovolcanoes directly overlying subvolcanic intrusions (e.g., Bodie-Aurora Hills, Chesterman and Gray, 1975; Breit et al., 1995; Virginia Range, Thompson, 1956; Vikre, 1989a; Hudson, 1993), an environment also conducive for the formation of porphyry copper deposits (Tosdal and Richards, 2001). In contrast, the bimodal assemblage was erupted during continental rifting under conditions of high differential horizontal stress and a moderate extension rate, and, except for the initial stages of this magmatic assemblage, magma supply rates probably were lower than for the western andesite assemblage. In this tectonic environment, extensional faults allowed rapid ascent of mafic magmas from the lithosphere, leading to formation of monogenetic volcanoes and elongate or elliptical, subvolcanic intrusions and strongly aligned dike swarms (Fig. 9; e.g., central northern Nevada rift; John et al., 2000).

Although magmatic activity spanned considerable time in both assemblages, individual volcanic centers in the western andesite assemblage generally were much longer lived than those in the bimodal assemblage (Table 2). Typical volcanic fields in the western andesite assemblage were active for 3 to 8 m.y., although compositions and loci of eruptions within individual fields varied through time. In contrast, magmatic centers in the bimodal assemblage were seldom active for more than 1 to 2 m.y., and many of the mafic rocks were not erupted from magmatic centers.

Comparison of the compositional characteristics of suites of rocks from the two magmatic assemblages highlight systematic differences between them (Figs. 4–7, Table 3). The bimodal assemblage is a K-rich tholeiitic series using classification schemes of Irvine and Baragar (1971) and Miyashiro (1974; Figs. 4 and 5). Intermediate and silicic rocks are noteworthy for their extremely low Mg and high Fe contents, and their compositions show a strong Fe enrichment trend (Mg no., Table 3; John et al., 1999). These rocks are highly enriched in large ion lithophilic elements (K, Rb, Ba), Th, rare earth elements, and high field strength elements (Ti, Nb, Ta, Y, Zr), and they have low Sr contents. In contrast, rocks from the western andesite assemblage do not show an Fe enrichment trend, have relatively low Ti, Nb, Ta, Y, and Zr contents, and have high Ba/Nb, Ba/La, K/La, Ba/Ta, and Zr/Nb ratios typical of subduction-related calc-alkaline magmas (Table 3; Gill, 1981; Luhr, 1992; Davidson and de Silva, 1995).

Rocks of the western andesite assemblage probably were generated by partial melting of the mantle wedge above subducting oceanic lithosphere of the Farallon plate (Fig. 10). Compositional characteristics of this assemblage indicate that melting was enhanced by volatile flux from the subducting plate, resulting in oxidized, water-rich magmas enriched in K, Rb, Sr, and Ba relative to high field strength elements. These magmas were emplaced mostly into the Walker Lane belt.

Mafic rocks of the bimodal basalt-rhyolite assemblage generally have compositions and isotopic characteristics, suggesting formation from a subduction-enriched lithospheric mantle source (Fig. 10; Fitton et al., 1991). The silicic rocks probably were produced by small amounts of partial melting of the lower crust, resulting from underplating by basaltic magmas (Honjo et al., 1992). Sparse intermediate compositions may be the result of mixing of basalt and rhyolite magmas facilitated by extensional faulting, as suggested by Johnson and

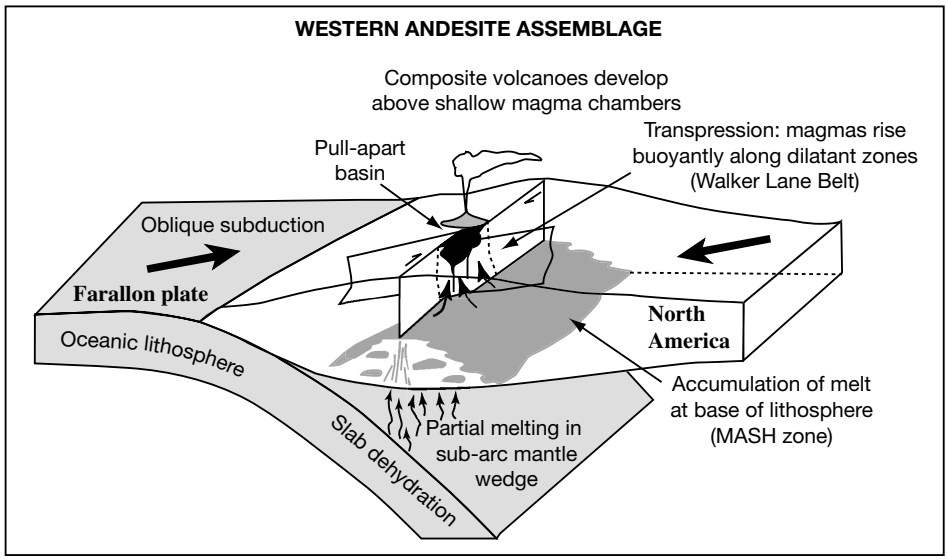

FIG. 10. Model for the magmatic-tectonic setting of the western andesite assemblage. Along the western side of the Great Basin, oblique subduction of oceanic lithosphere (Farallon plate) beneath North America was occurring. Downgoing oceanic crust dehydrated, releasing volatiles that facilitated partial melting of the mantle wedge. These volatile-rich mafic melts rose buoyantly to the base of the lithosphere and ponded in the MASH zone (melting, assimilation, storage, and homogenization; Hildreth and Moorbath, 1988), where they extensively interacted with the lower crust and probably formed diffuse batholiths. Transtensional zones and pull-apart basins developed locally due to strike-slip faulting parallel to the arc and allowed the hydrous magmas to rise buoyantly to shallow crustal levels and further fractionate and interact with the crust. Some of these magmas erupted, forming polygenetic stratovolcanoes directly over the shallow magma chambers. Modified from Tosdal and Richards (2001).

Grunder (2000) for rocks of intermediate composition in the 10.4 Ma bimodal suite in southeast Oregon.

Miocene and Early Pliocene Epithermal Gold-Silver Deposits in the Northern Great Basin

Epithermal gold-silver deposits of Miocene to early Pliocene age are abundant in the northern Great Basin and include the world-class Comstock Lode, Goldfield, Tonopah, and Ken Snyder (Midas) deposits (Fig. 2b and c). These deposits can be broadly separated into two groups, high-sulfidation (acid-sulfate) and low-sulfidation (adularia-sericite types), based on their ore assemblages and associated hydrothermal alteration (Table 4; Heald et al., 1987; White and Hedenquist, 1990; Hedenquist et al., 2000). Both deposit types are abundant in the northern Great Basin (Fig. 2b and c). As discussed below, ore assemblages suggest that low-sulfidation deposits in the western andesite assemblage have oxidation and sulfidation states transitional between the low-sulfidation deposits in the bimodal assemblage and high-sulfidation deposits. This observation has led to subdivision of low-sulfidation deposits into two subtypes (types 1 and 2 of John et al., 1999; intermediate-sulfidation and end-member low-sulfidation types of Hedenquist et al., 2000), based on characteristics of ore assemblages, metal contents and ratios, and volcano-tectonic setting (Tables 4 and 5; Albino and Margolis, 1991; Margolis, 1993; John, 1999, 2000; John et al., 1999; Hedenquist et al., 2000). Low-sulfidation deposits in the bimodal assemblage formed in an extensional (rift) environment and most commonly were associated with rhyolitic flows and domes of the bimodal basalt-rhyolite assemblage. Low-sulfidation deposits in the western andesite assemblage formed in constructional volcanic settings, commonly in zones of strike-slip faulting, and generally were associated with andesite and/or dacite stratovolcanoes and dome fields.

In the northern Great Basin, high-sulfidation deposits are restricted to the western andesite assemblage, whereas low-sulfidation deposits with variable characteristics are present in both magmatic assemblages (Table 5; Fig. 2b and c). Most low-sulfidation deposits in the bimodal assemblage formed in two distinct settings (Table 4; John et al., 1999): hosted by, or spatially and temporally associated with, rhyolite flow domes and flow sequences (e.g., Sleeper, DeLamar, National, Jarbidge) or associated with mafic flows and dikes of the northern Nevada rift (e.g., Mule Canyon, Buckhorn). In addition, several shallow-depth, low-sulfidation deposits of Pliocene(?) age are hosted by clastic sedimentary rocks. These deposits are younger than most other epithermal deposits in the northern Great Basin, explaining the preservation of hot-spring features, and appear to be unrelated to magmatism (e.g., Sulphur (Crofoot-Lewis), Ebert et al., 1996; Wind Mountain, Wood, 1991). A few epithermal deposits also are present in late Eocene to early Miocene caldera-related volcanic centers of the interior andesite-rhyolite assemblage (Fig. 2a), most notably the huge, late Oligocene low-sulfidation deposit at Round Mountain; these deposits are not discussed in this paper.

Deposit characteristics

Characteristics of low-sulfidation deposits vary significantly reflecting fundamental differences in their environments of formation and associated magmatism (Table 4; John, 1999, 2000; John et al., 1999). Some important differences include: (1) tectonic setting; (2) characteristics of associated igneous rocks and possible relationship to magmatism; (3) duration of associated magmatism and hydrothermal activity; (4) areal extent of hydrothermal systems and hydrothermal alteration; (5) other types of associated deposits; (6) geochemical characteristics, metal contents, and metal ratios of ores; (7) ore mineralogy; (8) inferred sulfidation and oxidation states of ore fluids; and (9) stable isotope composition, salinity, and gas content of ore fluids.

Tectonic setting of magmatism and epithermal deposits: Eruption of much of the western andesite assemblage may have been localized in transtensional zones related to strike-slip faults in the Walker Lane belt (e.g., Breit et al., 1995; Berger and Drew, 1997; Berger et al., 1999). Similarly, many epithermal and porphyry systems in the western andesite assemblage may have been localized in extensional duplexes and releasing bends related to these strike-slip faults (e.g., Borealis, Eng, 1991; Haney et al., 2000; Rawhide, Black et al., 1991, Gray, 1996; Santa Fe, Albino and Boyer, 1992; Bodie-Aurora, Berger et al., 1999; Breit et al., 1995; B. Maher, oral commun., 2001; Goldfield, Berger and Drew, 1997; Comstock Lode, Berger, 1996). Although several epithermal deposits in the western andesite assemblage may have formed during large-magnitude Miocene extension (e.g., Tonopah, Seedorff, 1991), most deposits are associated with rocks erupted after large-magnitude extension, as shown by pronounced angular unconformities, during periods of more moderate extension possibly related to strike-slip faulting of the Walker Lane belt.

In contrast, the bimodal basalt-rhyolite assemblage was erupted in an extensional environment during continental rifting. The types of eruptions and orientations of dikes and shallow intrusions in this assemblage are consistent with an extensional tectonic environment that allowed rapid ascent of mafic magmas from the upper mantle (see above), and little evidence is present for strike-slip faulting during the early (ca. 17–10 Ma) stages of magmatism when most epithermal deposits in this assemblage formed. Although small amounts of oblique-slip displacement have been documented for a few epithermal deposits in the bimodal assemblage (e.g., Ken Snyder deposit, Midas district; Goldstrand and Schmidt, 2000), displacement on most faults controlling mineralization appears to be dominantly dip-slip (e.g., Sleeper, Nash et al., 1995; Mule Canyon, John and Wallace, 2000), and strike-slip faults do not appear to have played a major role in the formation of most epithermal deposits in the bimodal assemblage.

Associated igneous rocks and relationship to magmatism: Epithermal gold-silver deposits in the western andesite assemblage generally have close spatial, temporal, and genetic links to magmatism, as shown by field relationships, geochronology, stable isotope data, alteration zonation, temperatures of hydrothermal mineral assemblages, and salinities and gas contents of ore fluids (e.g., Comstock Lode, Goldfield, and Paradise Peak: Taylor, 1973; Ashley, 1974, 1979; Vikre et al., 1988; Vikre, 1989a, b; John et al., 1989, 1991; Rye et al., 1992; Sillitoe and Lorson, 1994). The advanced argillically altered hosts to high-sulfidation deposits, such as Goldfield and Paradise Peak, are inferred to have formed from

TABLE 4. Characteristics of Miocene and Early Pliocene Epithermal Gold-Silver Deposits in the Northern Great Basin

Deposit type	High-sulfidation	Low-sulfidation	Low-sulfidation
Alternative deposit types	Acid-sulfate[1]	Adularia-sericite,[1] type 1 low-sulfidation,[2] intermediate-sulfidation[2]	Adularia-sericite,[1] type 2 low-sulfidation,[2] end-member low-sulfidation[3]
Igneous association	Western andesite	Western andesite	Bimodal
Igneous setting	Andesite/dacite stratovolcanoes and dome fields in subduction-related continental margin volcanic arc	Andesite/dacite stratovolcanoes and dome fields in subduction-related continental margin volcanic arc	Rhyolite domes; mafic dikes intruding mafic volcanic piles and volcaniclastic sedimentary rocks
Tectonic setting	Transtensional zones related to strike-slip faults	Transtensional zones related to strike-slip faults	Extensional faults related to continental rifting
Mineralization style	Residual ("vuggy") silicified zones and quartz veins locally containing pods of massive sulfides; hydrothermal/tectonic breccias	Vuggy, often rhythmically banded and comb texture veins; mineralized zones generally ≤10 m wide, may be continuous for kilometerss along strike and up to 1 km downdip; repeated fault brecciation	Narrow (≤2 m wide), rhythmically banded silica ±calcite ±adularia veins; veins may extend along strike for several kilometerss; hydrothermal/ tectonic breccias; repeated fault brecciation
Hydrothermal alteration	Widespread propylitic alteration; inner zones of vuggy silica, advanced argillic (kaolinite/ dickite, diaspore, pyrophyllite, andalusite), alunitic, and sericitic alteration; barren lithocaps of silicification	Regional propylitic alteration (calcite-chlorite ± epidote); narrow zones of superimposed adularia, sericite, and argillic alteration around quartz ± carbonate ± adularia veins; barren steam-heated argillic alteration overlying boiling zones	Narrow zones of argillic (smectite/illite) alteration; inner zones of silica-illite ± adularia; silica is mostly opal or chalcedony; local peripheral propylitic alteration (calcite-chlorite ± epidote); barren steam-heated argillic alteration overlying boiling zones
Metals produced	Au, Ag ±Cu	Au, Ag ±Cu, Pb, Zn	Au, Ag ±Hg
Geochemical signature	Au, Ag, As, Sb, Pb, ±Bi, Cu, Hg, Mo, Sn, Te, Zn	Au, Ag, Ba, Mn, ±Cu, Pb, Se, Zn	Au, Ag, As, Sb, Se, Hg, ±Mo, Tl, W
Ag/Au	Generally low, 1:5 to 2:1 (Paradise Peak is anomalously high 15:1)	High, generally 10:1 to 100:1	Moderate, generally 2:1 to 10:1 (bonanza veins at Sleeper about 1:1)
Base metal content (Cu + Pb + Zn)	Generally high; Cu production in some districts	Variable, but generally >200 ppm	Low, generally ≤200 ppm
Ore mineralogy	Pyrite, gold, enargite/luzonite, sphalerite, covellite, ±chalcopyrite, galena, tetrahedrite/ tennantite, bismuthanite, stibnite, Au tellurides	Pyrite, electrum, silver sulfides and sulphosalts; local sphalerite, galena, chalcopyrite	Pyrite/marcasite, arsenopyrite, electrum, gold, Ag selenides and sulfides, stibnite, local pyrrhotite, minor local sphalerite, galena, chalcopyrite, tetrahedrite, Se sulphosalts
Gangue mineralogy	Quartz, opal, chalcedony, barite, local alunite, kaolinite	Quartz, carbonate, sericite ± adularia, rare chlorite	Opal-chalcedony, quartz, illite/sericite, ±adularia, ±carbonate, ±montmorillinite
Sulfide content	High	Variable, can be high in deeper parts of systems (30%)	Variable, but generally low (<1%); deposits hosted by mafic rocks of the northern Nevada rift may contain up to 30% Fe sulfide
Ore fluids	Low pH, high f_{O_2} and f_{S_2}, variable salinity (deep halite-saturated fluids)	Neutral pH, low to moderate f_{O_2} and f_{S_2}, low to moderate salinities (1–6 wt % NaCl equiv), locally CO_2 rich	Neutral pH to slightly acidic, low f_{O_2} and f_{S_2}, low salinity (≤2 wt % NaCl equiv)
Temperature of ore formation	<200° (Paradise Peak, Borealis) to >300°C (Goldfield)	200° to 280°C	Generally ≤200°C (deposits in the National district and parts of the Midas district to approx 300°C)

[1]Heald et al. (1987)
[2]John et al. (1999)
[3]Hedenquist et al. (2000)

TABLE 5. Miocene and Early Pliocene Epithermal Gold-Silver Deposits in the Northern Great Basin

Western andesite assemblage		Bimodal basalt-rhyolite assemblage	
Low-sulfidation	High-sulfidation	Low-sulfidation	Low-sulfidation, nonmagmatic
Aurora	Borealis	Buckhorn	Florida Canyon(?)
Bodie	Golden Dome	Bullfrog	Sulphur (Crofoot-Lewis)
Como	Goldfield	Delamar	Wind Mountain
Comstock Lode	Masonic	Fire Creek	
Divide	Morningstar (Monitor district)	Goldbanks	
Gilbert	Paradise Peak	Grassy Mountain	
Gooseberry	Peavine-Wedekind	High Grade	
Hasbrouck Mountain	Ramsey-Comstock	Hog Ranch	
Olinghouse	Santa Fe	Ivanhoe	
Silver Peak		Jarbidge	
Talapoosa		Manhattan(?)	
Tonopah		Midas	
Zaca (Monitor district)		Mountain View	
		Mule Canyon	
Interior andesite assemblage		National	
		Quartz Mountain	
Low-sulfidation		Rock Creek	
Atlanta(?)		Seven Troughs	
Bell Mountain		Sleeper	
Faiview		Tenmile	
Round Mountain			
Tuscarora			
Wonder			

condensation of magmatic vapor (Vikre, 1989b; Rye et al., 1992; also see reviews by Hedenquist and Lowenstern, 1994; Arribas, 1995), followed by a magmatic liquid that deposits ore (Hedenquist et al., 1998). Hydrothermal fluids that formed bonanza ores at the Comstock Lode also appear to have had a significant magmatic component (Taylor, 1973; O'Neil and Silberman, 1974; Vikre, 1989a, Simmons, 1995). In contrast, epithermal deposits in the bimodal assemblage generally are spatially and temporally associated with volcanism, but their genetic relationship to magmatism is less certain (e.g., National district, Vikre, 1985, 1987; Sleeper, Nash et al., 1995; Saunders and Schoenly, 1995).

As discussed above, magmas of the western andesite assemblage were relatively water rich and oxidized, which are characteristics typical of subduction-related calc-alkaline volcanic arcs that generate porphyry copper-gold deposits throughout the Circum-Pacific (e.g., Burnham, 1979; Burnham and Ohmoto, 1980; Hedenquist and Lowenstern, 1994; Sillitoe, 2000). Rocks in this assemblage are similar in composition to those that formed high-sulfidation deposits elsewhere and are distinct from the sparse intermediate composition rocks of the bimodal assemblage (Table 3, Fig. 7; Arribas, 1995). In contrast, magmas of the bimodal assemblage had low water contents and low oxygen fugacities, and silicic magmas probably were strongly contaminated by crustal materials (Honjo et al., 1992; John et al., 2000). Hydrothermal systems related to these magmas can form deposits enriched in lithophile elements (Li, Cs, Rb), Hg, Be, and U (e.g., McDermitt caldera complex, Rytuba and Glanzman, 1979). These magmas also can be affiliated with reduced Mo-Sn-W-rich porphyry systems, such as the Izzenhood and Ivanhoe Sn-bearing rhyolites (Fries, 1942; Wallace and John, 1998).

Duration of magmatism and hydrothermal activity: The western andesite assemblage was characterized by long-lived, polygenetic stratovolcanoes and dome fields (Tables 1 and 2). Eruptions within volcanic centers, such as those in the Virginia Range and in the Bodie Hills, may have spanned a period of 7 to 10 m.y., and hydrothermal systems forming epithermal gold-silver deposits and porphyry-style altered and low-grade base and precious metal mineralized rocks in these areas most likely were active repeatedly during much of the life span of the magmatism (Table 2). In contrast, the bimodal assemblage was characterized by much shorter lived, monogenetic volcanic fields consisting mostly of mafic cinder cones, sheet flows, and dike swarms and silicic domes. Individual volcanic centers seldom were active for more than 1 to 2 m.y. (Tables 1 and 2). Most hydrothermal activity that formed epithermal deposits in the bimodal assemblage occurred during a brief time interval between about 16 and 14 Ma that corresponded to the peak of magmatic activity in this assemblage in the northern Great Basin (Noble et al., 1988; McKee and Moring, 1996; John et al., 1999). In contrast, epithermal deposits in the western andesite assemblage formed throughout the duration of magmatism, between about 21 to 4 Ma (Silberman et al., 1976; McKee and Moring, 1996; John et al., 1999).

Areal extent of hydrothermal systems and hydrothermal alteration: Regional-scale propylitic alteration affected large areas of the western andesite assemblage. This alteration was developed most prominently around the Comstock Lode in the Virginia Range and in the Markleeville area (Monitor district) in eastern California, where more than 100 km^2 of middle Miocene volcanic rocks and Mesozoic basement rocks underwent strong propylitic alteration (Coats, 1940; Wilshire, 1957; Whitebread, 1976; Vikre, 1989a). In these districts,

small (less than a few square kilometers) areas of other types of hydrothermal alteration were widely distributed and superimposed on the regional propylitic alteration. In contrast, regional-scale propylitic alteration did not develop in bimodal assemblage rocks, and alteration zones tend to be narrow and largely restricted to wall rocks immediately adjacent to the faults that channeled ore-forming hydrothermal fluids (John et al., 1999; John and Wallace, 2000; Leavitt et al., 2000a).

The regional-scale propylitic alteration in the western andesite assemblage was probably a function of the style and duration of magmatic activity (long-lived stratovolcanoes and abundant subjacent volatile-rich intrusions). These volcanic centers most likely had substantial topographic relief with large hydraulic heads to recharge ground water. The large hydraulic gradients, combined with numerous shallow intrusions, resulted in large, long-lived and extensive hydrothermal systems. In contrast, most volcanic centers in the bimodal assemblage were relatively short lived, and volatile-rich subvolcanic intrusions were uncommon. For example, magmatic activity around the Mule Canyon deposit in the bimodal assemblage probably spanned no more than 1.7 m.y., with most igneous and hydrothermal activity occurring within about 800,000 yr (Table 2). Most lava flows here are thin, and despite the location of the deposit along of the western side of the northern Nevada rift, substantial relief apparently was absent (John et al., 2000).

Other associated mineral deposits: In the western andesite assemblage, high-sulfidation deposits are present in many districts containing low-sulfidation deposits (Fig. 2b), and it has been suggested that porphyry copper-gold deposits may underlie high-sulfidation deposits in several districts, including the Goldfield, Monitor, Peavine-Wedekind, and Golden Dome districts (Fig. 2b; Hudson, 1977, 1983; Wallace, 1979; Albino, 1991; Canby, 1992; Rytuba, 1996). Sillitoe and Lorson (1994) noted alteration patterns characteristic of a porphyry gold system several kilometers west of the Paradise Peak high-sulfidation deposit, and Hollister and Silberman (1995) suggested that porphyry copper-gold mineralization may underlie gold-rich polymetallic veins in the Bodie district. Numerous porphyry copper deposits are present in more deeply eroded parts of the Miocene Cascades arc farther north, such as the Glacier Peak and Earl/Margaret (Mount St. Helens) deposits in Washington (Power, 1985; Derkey at al., 1990). In addition, stratiform sulfur replacement deposits genetically related to high-sulfidation deposits are present locally in eastern California and western Nevada in the western part of the arc (Rytuba, 1996; Vikre, 2000), notably at the Leviathan mine in the Monitor district (Evans, 1977). In contrast, no high-sulfidation or porphyry Cu-Au deposits are known in the bimodal assemblage. Because of the low water contents, reduced nature, and deep emplacement of the magma chambers, there is little likelihood that these types of deposits are present in bimodal assemblage rocks (see below; John et al., 1999).

Geochemical characteristics, metal contents, and metal ratios of ores: Geochemical characteristics, Ag/Au ratios, and base metal contents of low-sulfidation deposits vary significantly within deposits, between deposits, and between magmatic assemblages. In general, however, ores in low-sulfidation deposits in the bimodal assemblage have significantly greater As, Hg, Sb, Se, and Tl contents, lower Ag/Au ratios, and lower base metal contents (Cu + Pb + Zn) than low-sulfidation deposits in the western andesite assemblage (Table 4; John et al., 1999). Ores in low-sulfidation deposits in the western andesite assemblage commonly have greater Ba, Mn, and Te contents than deposits in the bimodal assemblage. Silver/gold ratios of the bimodal assemblage deposits typically are <10 and are near 1 in many deposits (Long et al., 1998; John et al., 1999). In contrast, Ag/Au ratios generally are >10 in low-sulfidation deposits in the western andesite assemblage, and deposits such as Comstock Lode and Tonopah averaged 23 and 94, respectively (Bonham, 1969; Bonham and Garside, 1979). Base metal contents (Cu + Pb + Zn) generally are low in low-sulfidation deposits in the bimodal assemblage, seldom exceeding 200 ppm (e.g., Vikre, 1985; Monroe et al., 1988; Nash et al., 1995; Bussey, 1996; John and Wallace, 2000). Base metal contents generally are higher in low-sulfidation deposits in the western andesite assemblage, commonly >500 ppm Cu + Pb + Zn, and parts of the northern bonanza in the Comstock Lode exceeded 30 wt percent sphalerite, galena, and chalcopyrite (Vikre, 1989a). However, a few low-sulfidation deposits in the western andesite assemblage that are associated with rhyolitic volcanism have notably low base metal contents (e.g., Aurora, Osborne, 1991; B. Maher, writ. commun., 2000; Rawhide, Black et al., 1991; Gray, 1996). Ores in high-sulfidation deposits in the western andesite assemblage generally contain still higher Cu + Pb + Zn contents, and by-product copper was produced from several districts (Goldfield, Masonic, Peavine-Wedekind, Fig. 2b).

Ore mineralogy: Ore mineralogy is one of the most distinctive differences between the low-sulfidation deposits in the two magmatic assemblages (Tables 4 and 6). Nearly all low-sulfidation deposits in the bimodal assemblage contain abundant silver selenide minerals (generally naumanite, Ag_2Se,

TABLE 6. Ore Mineral Characteristics of Miocene and Early Pliocene Low-Sulfidation Gold-Silver Deposits, Northern Great Basin (common, present in most deposits; uncommon, present in a few deposits)

Mineral	Western andesite assemblage	Bimodal assemblage
Pyrite	Ubiquitous	Ubiquitous
Marcasite	Rare	Common
Pyrrhotite	Rare or absent	Uncommon
Arsenian pyrite/ marcasite	Absent	Uncommon
Arsenopyrite	Rare or absent	Common
Silver sulfides	Ubiquitous	Common
Silver sulfosalts	Common	Uncommon
Silver selenides	Rare	Ubiquitous
Electrum	Common	Common (commonly dendritic)
Chalcopyrite	Common	Common (trace amounts)
Tetrahedrite/ tennantite	Common	Uncommon (trace amounts)
Stibnite	Uncommon	Common
Galena	Common	Uncommon (trace amounts)
Sphalerite	Common (Fe-poor)	Uncommon (trace amounts, Fe-rich, inhomogeneous)
Hematite	Rare	Absent

and/or aguilarite, Ag_4SeS). In contrast, silver selenide minerals are rare to absent in low-sulfidation deposits in the western andesite assemblage, but significant Se may be incorporated into tetrahedrite or other sulfosalts (e.g., Comstock Lode, Vikre, 1989a; Gooseberry, Perkins, 1987) or in acanthite. For example, acanthite in the Comstock Lode contains 1 to 10 mole percent Se (Vikre, 1989a), and acanthite from Tonopah contains 1 to 8 mole percent Se (D.A. John, unpub. data, 2000). Other mineralogical differences include marcasite, which is abundant in most deposits in the bimodal assemblage but absent in low-sulfidation deposits in the western andesite assemblage, arsenopyrite, which is abundant in many deposits in the bimodal assemblage but generally absent in deposits in the western andesite assemblage, and pyrrhotite, which is present in several deposits in the bimodal assemblage but typically absent in deposits in the western andesite (Table 6; John et al., 1999). Stibnite (or berthierite, Vikre, 1985) is present in many low-sulfidation deposits in the bimodal assemblage, whereas Sb is incorporated mostly into tetrahedrite or other sulfosalts in low-sulfidation deposits in the western andesite. Sphalerite in deposits in the bimodal assemblage tends to be Fe rich and compositionally zoned, whereas sphalerite in low-sulfidation deposits in the western andesite assemblage is Fe poor and compositionally homogenous (Table 7; P.G. Vikre, writ. commun., 2000; see below).

Relative oxidation and sulfidation states of ore assemblages: Ore mineral assemblages and mineral compositions suggest that low-sulfidation deposits in the western andesite assemblage generally formed at higher sulfur and oxygen fugacities than low-sulfidation deposits in the bimodal assemblage and are transitional with high-sulfidation deposits (Figs. 11 and 12; John et al., 1999; Hedenquist et al., 2000). Relatively few detailed studies of ore assemblages and ore fluids for epithermal deposits in the northern Great Basin exist; consequently, a rigorous evaluation of sulfidation and oxidation states of ore assemblages and ore fluids is not attempted here. Vikre's studies of deposits in the National district (1985) in the bimodal assemblage and of the Comstock Lode (1989a) in the western andesite assemblage are two of the most complete studies. Comparison of the Comstock Lode to the National district indicates that bonanza ores in the Comstock Lode formed at higher oxygen and sulfur fugacities than ores in the National district (Figs. 11 and 12). Reconnaissance studies of other deposits in the western andesite assemblage (Bodie, Tonopah, and Zaca mine, Monitor district) and in the bimodal assemblage (Mule Canyon, Rosebud, and Buckhorn) also support this distinction in oxygen and sulfur fugacities (Figs. 11 and 12, Tables 4 and 7). Lower sulfur and oxygen fugacities for low-sulfidation deposits in the bimodal assemblage also are suggested by the presence of pyrrhotite and/or arsenopyrite and by the ubiquitous presence of silver selenides in these deposits and the incorporation of Se into sulfosalts rather than into selenide minerals in deposits in the western andesite assemblage (Margolis, 1993; Simon et al., 1997). The generally low Fe contents of sphalerite (Table 7), the occurrence of tetrahedrite-tennantite, and the local presence of hematite and/or Fe-rich chlorite in ore assemblages (e.g., Aurora; Osborne, 1991) in low-sulfidation deposits in the western andesite assemblage also indicate higher oxygen and sulfur fugacities than in deposits in the bimodal assemblage. The presence of stibnite and local berthierite rather than tetrahedrite in many low-sulfidation deposits in the bimodal assemblage also may indicate lower sulfur fugacities (Seal et al., 1990).

Stable isotope composition, salinity, and gas content of ore fluids: Available fluid inclusion data indicate that the low-sulfidation deposits in the bimodal assemblage have very low salinity ore fluids. Such low-salinity fluids were incapable of transporting significant quantities of silver and base metals (Henley, 1990), explaining their generally low contents in these ores. For example, ore-stage fluids in the National district had maximum salinities of 1.3 wt percent NaCl equiv

TABLE 7. Iron Contents of Sphalerite in Miocene and Early Pliocene Epithermal Deposits, Northern Great Basin

Sample no.	No. analyses[1]	X_{Fe}(min)[2]	X_{Fe}(max)[2]	Mineral assemblage[3]
Tonopah (Belmont mine)				
Tonopah 1A	17	0.2	1.2	qtz-ill-calcite-py-spl-cp-gl
Tonopah E4-B	48	0.2	1.7	qtz-ill-py-spl-gl-el-acan
Bodie (Red Cloud mine)				
99-DJ-72E	11	0.3	1.7	qtz-ill-cp-spl-tet-py-el-hessite
99-DJ-72D	9	0.4	2.0	qtz-ill-cp-spl-py-tet-gl
Zaca mine				
D-6	17	0.7	2.1	qtz-Ksp-ill-py-cp-spl-tet-gl-mo
D-8	31	0.5	1.5	qtz-Ksp-ill-py-cp-spl-tet-gl
Rosebud mine				
Rosebud 1	19	3.3	13.7	qtz-ill-dickite-mc-cp-tet-spl-asp-el
Rosebud 3b	6	0.8	13.5	qtz-ill-py-tet-spl-cp-el-gl
Mule Canyon mine				
97-MC-1	1	10.0	10.0	qtz-ad-ill-py-mc-asp-spl

[1] Number of electron microprobe analyses

[2] Fe/(Fe + Zn), in mole percent

[3] Mineral abbreviations: acan = acanthite, ad = adularia, asp = arsenopyrite, cp = chalcopyrite, el = electrum, gl = galena, ill = illite, Ksp = K feldspar, mc = marcasite, mo = molybdenite, py = pyrite, qtz = quartz, spl = sphalerite, tet = tetrahedrite

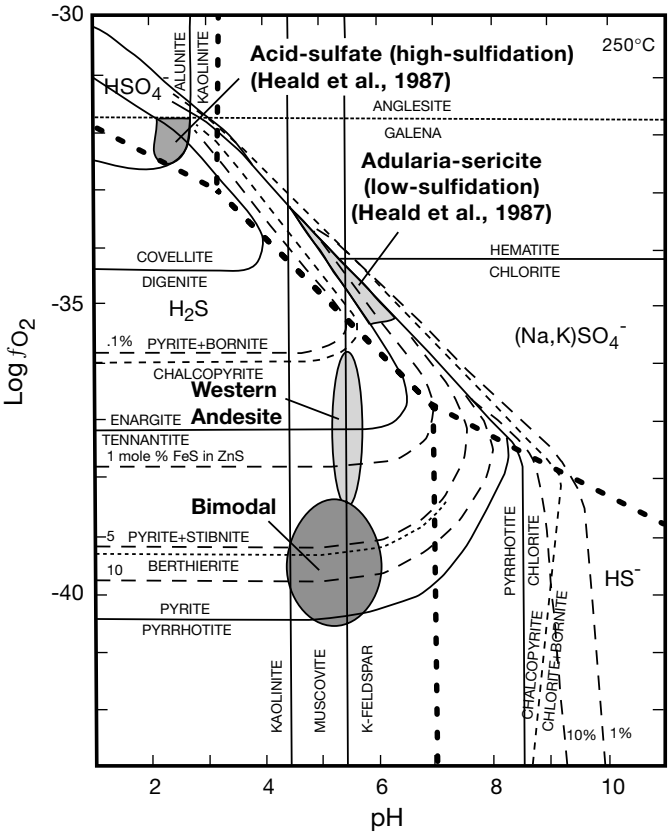

FIG. 11. Log f_{O_2}-pH diagram at 250°C, total sulfur = 0.02 *m*, and salinity = 1 *m* with Na/K = 9. Modified from Heald et al. (1987). Dotted curve showing berthierite stability from Barton and Skinner (1979). Fields inferred for ore fluids for low-sulfidation deposits in the western andesite and bimodal assemblages based on ore assemblages and compositional data for the National district from Vikre (1985), data for the Comstock Lode from Vikre (1989a), and reconnaissance data for Tonopah, Bodie, Zaca, Rosebud, Mule Canyon, and Buckhorn collected as part of this study (see text). Fields for acid-sulfate and adularia-sericite deposits from Heald et al. (1987). Ore fluids for adularia-sericite deposits are assumed to be in equilibrium with Fe-rich chlorite and hematite. Ores in most low-sulfidation deposits in the northern Great Basin lack these minerals, suggesting lower oxidation states.

(Vikre, 1985a), bonanza ore fluids at Sleeper had salinities of 0.1 to 0.6 wt percent NaCl equiv (Saunders and Schoenly, 1995), and bonanza vein fluids at Midas had salinities of about 0.5 to 0.6 wt percent NaCl equiv (Blair, 1991; Goldstrand and Schmidt, 2000; Ioannou and Spooner, 2000). In contrast, limited data for ore fluids in the western andesite assemblage suggest somewhat higher salinities, including some bonanza ore fluids at the Comstock Lode with salinities as much as 6 wt percent NaCl equiv (Vikre, 1989a), ore fluids at Aurora with 2 to 6 wt percent NaCl equiv (Osborne, 1991), and ore fluids at Tonopah with 0.8 to 2.0 wt percent NaCl equiv (Fahley, 1979), although the possible effect of dissolved CO_2 in inclusion fluids on calculated salinities (Hedenquist and Henley, 1985) is not discussed in these studies. At DeLamar, a low-sulfidation deposit in the bimodal assemblage that has an anomalously high Ag/Au ratio of 40, late-stage ore fluids had salinities of 2.8 to 3.8 wt percent NaCl equiv (Halsor et al., 1988), so the high Ag contents there may correspond to relatively high salinity ore fluids.

Sparse gas analyses of fluid inclusions suggest that ore-stage fluids in low-sulfidation deposits in the western andesite assemblage (Comstock Lode, Tonopah) may have had larger dissolved gas contents than ore fluids in low-sulfidation deposits in the bimodal assemblage (National, Sleeper, Dixie prospect of the Midas district; Vikre, 1985, 1989a; Graney and Kesler, 1995; Saunders and Schoenly, 1995; Ioannou and Spooner, 2000).

Stable isotope analyses of ores from low-sulfidation deposits in the bimodal and western assemblage assemblages show that both deposit types were dominated by meteoric waters over the life of the systems (O'Neil et al., 1973; Taylor, 1973; O'Neil and Silberman, 1974; Vikre, 1987, 1989a). However, ore fluids in bonanza parts of the Comstock Lode appear to have had a significant magmatic component (30–75%). Such evidence has not been found to date in most other deposits (Taylor, 1973; Vikre, 1989a; Simmons, 1995).

Discussion

Most Miocene and early Pliocene epithermal gold-silver deposits of the northern Great Basin are spatially and temporally related to two distinct magmatic assemblages that formed in differing tectonic settings (Figs. 11 and 12). Types and characteristics of epithermal deposits vary systematically between the two magmatic assemblages, suggesting that magmas may have played a fundamental role in the genesis of these deposits. The differences described here between types of epithermal deposits could arise from (1) variable basement and/or volcanic wall rocks, (2) variable tectonic and hydrologic environments of magmatism and ore formation, (3) variable amounts and/or types of magmatic input to ore-forming fluids, or (4) most likely, a combination of the above.

Effects of basement and volcanic wall rocks

Although basement terranes and the types of rocks in these terranes vary significantly across the Great Basin (Fig. 3; Stewart and Carlson, 1978; Ludington et al., 1996a), basement rocks do not vary significantly between the two major Miocene magmatic assemblages. Furthermore, the continental margin of North America, as inferred from the initial $^{87}Sr/^{86}Sr$ = 0.706 isopleth, crosses the bimodal and western andesite assemblages and does not correlate with the types of epithermal deposits present in these assemblages (Fig. 2b and c). These relationships suggest that variations in the types and characteristics of the epithermal deposits in the two magmatic assemblages are not related primarily to variations in the types of basement rocks.

Variations in the oxidation state of volcanic wall rocks and preore-stage hydrothermal alteration may influence the characteristics of the epithermal deposits. In volcanic rocks of the bimodal assemblage, propylitic alteration is limited, probably reflecting the absence of large, long-lived, volatile-rich stratovolcanoes and the resulting lack of large hydrothermal systems driven by shallow intrusions. Relatively small volumes of reduced ore fluids flowing through relatively reduced wall rocks resulted in the maintenance of reduced conditions throughout the hydrothermal system. In contrast, large areas of relatively oxidized propylitic alteration form wall rocks of low-sulfidation deposits in the western andesite assemblage.

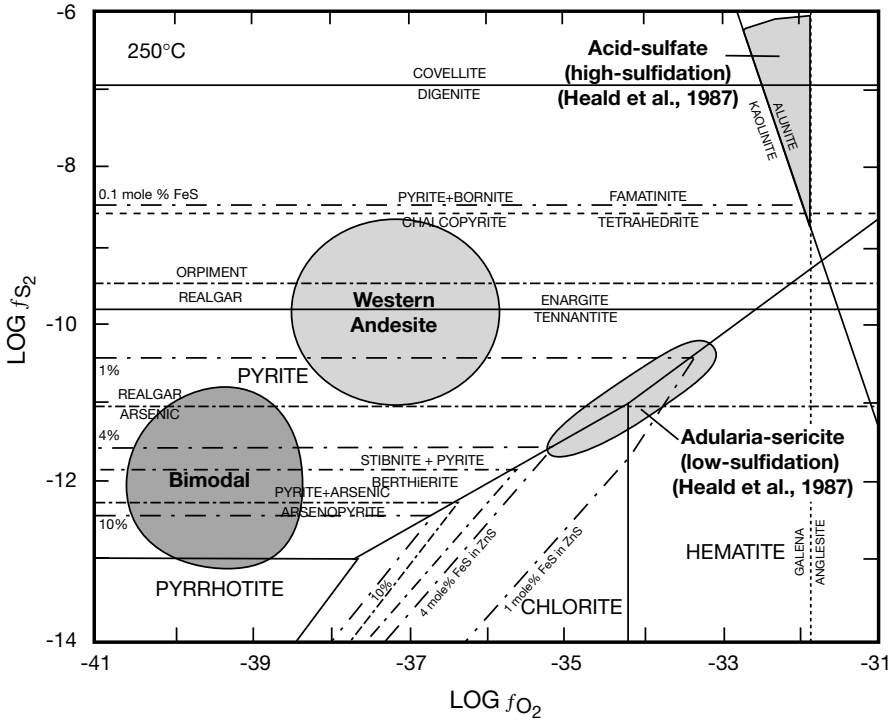

FIG. 12. Log δO_2-log δS_2 diagram at 250°C. Modified from Heald et al. (1987). Fields inferred for ore fluids for low-sulfidation deposits in the western andesite and bimodal assemblages based on ore assemblages and compositional data for the National district from Vikre (1985), data for the Comstock Lode from Vikre (1989a), and reconnaissance data for Tonopah, Bodie, Zaca, Rosebud, Mule Canyon, and Buckhorn collected as part of this study (see text). Berthierite and arsenic mineral stability curves calculated from equations in Barton and Skinner (1979). Kaolinite-alunite equilibrium drawn for pH = 2.8 and total sulfur = 0.02 *m*. Fields for acid-sulfate and adularia-sericite deposits from Heald et al. (1987). Ore fluids for adularia-sericite deposits are assumed to be in equilibrium with Fe-rich chlorite and hematite. Ores in most low-sulfidation deposits in the northern Great Basin lack these minerals, suggesting lower oxidation states.

The relatively oxidized ore fluids of the low-sulfidation deposits in the western andesite assemblage thus could reflect both the propylitized, relatively oxidized volcanic wall rocks and the direct input of oxidized magmatic fluids.

Effects of tectonic and hydrologic environments

The proportion and composition of magmatic components in deep geothermal fluids that can form epithermal gold-silver deposits may vary with tectonic environment. Giggenbach (1992b, 1995) suggested that the composition of deep geothermal fluids in the Taupo Volcanic Zone, New Zealand, is a function of their tectonic setting and source magmas. The eastern margin of the Taupo Volcanic Zone is characterized by subduction-related, arc-type andesitic magmatism. Deep geothermal fluids in this area have high CO_2 contents and high CO_2/Cl, $CO_2/^3$He, and N_2/Ar ratios. Based on relative contents of B, Cl, Li, and Cs, Giggenbach (1995) suggested that these deep geothermal fluids were derived from andesitic magmas and contained an average of about 14 percent magmatic component. The western portion of the Taupo Volcanic Zone is a rift environment undergoing crustal extension, and the bimodal basalt-rhyolite magmatism is dominated by silicic volcanism. Deep geothermal fluids here have lower CO_2 contents and lower CO_2/Cl ratios than geothermal systems in the eastern Taupo Volcanic Zone. Low $CO_2/^3$He and N_2/Ar ratios are consistent with mantle-derived volatiles, and Giggenbach (1995) estimated that these fluids contain only about 6 percent magmatic component. Giggenbach (1992c) estimated that geothermal systems in other subduction-related andesitic arcs, such as the Philippines, could contain as much as 50 percent magmatic water.

Geothermal systems in the Taupo Volcanic Zone are broadly analogous to hydrothermal systems thought to have formed epithermal gold-silver deposits worldwide (e.g., White, 1955, 1981; Henley and Ellis, 1983; Giggenbach, 1992a, 1997; Hedenquist and Lowenstern, 1994; Simmons and Browne, 2000). Although locally high concentrations of precious metals have been found in the eastern, arc-related Taupo Volcanic Zone geothermal systems, no economic quantities have yet been found. In the Taupo Volcanic Zone, both the rift-related rhyolitic magmas and arc-related andesitic magmas are calc-alkaline and relatively oxidized (magmatic oxygen fugacity ≥Ni-NiO buffer; Graham et al., 1995; Price et al., 1999), unlike the reduced, tholeiitic magmas of the bimodal assemblage in the northern Great Basin. Furthermore, mineralogical studies of drill core from the Broadlands geothermal system in the eastern part of the Taupo Volcanic Zone indicate relatively reduced hydrothermal fluids (low f_{O_2} and f_{S_2}) (Browne and Lovering, 1973), suggestive of bimodal, rift-related volcanism if hydrothermal fluid composition is influenced by magma composition. However, the variable amounts and types of magmatic input to geothermal systems in the

Taupo Volcanic Zone may be broadly characteristic of differing tectonic environments, continental rift-related bimodal magmatism versus subduction-related andesitic arc magmatism (Giggenbach, 1997), similar to the contrasting magmatic-tectonic environments in the Miocene Great Basin.

Magmatic contribution to ore-forming fluids and other components

The magmatic contribution, if any, to ore-forming fluids of most low-sulfidation deposits in the northern Great Basin remains ambiguous. The correlation between characteristics of the low-sulfidation deposits and magma composition and oxidation state suggests there may be a magmatic contribution to the ore-forming fluids. However, data critical to assess the magmatic contribution to these fluids, such as gas analyses of fluid inclusions and stable isotope analyses of ore-stage minerals, are sparse or lacking for most deposits.

Noble et al. (1988) and Connors et al. (1993) proposed that basaltic magmas of the bimodal assemblage were the primary source of gold, sulfur, and chloride in low-sulfidation deposits in the bimodal assemblage. They noted that the age of these deposits is restricted mostly between 16 to 14 Ma during the peak intensity of basaltic volcanism in the northern Great Basin, and that continental tholeiites, such as basaltic magmas in the bimodal assemblage, are relatively enriched in gold compared to more silicic rocks. Connors et al. (1993) showed that rhyolitic magmas of the bimodal assemblage and elsewhere generally have low gold contents and were unlikely sources for gold in the epithermal deposits in the bimodal assemblage. Noble et al. (1988) suggested that basaltic magmas of the bimodal assemblage provided the gold, sulfur, and chloride in the epithermal deposits in this assemblage, either directly from degassing of the magmas or by leaching of relatively gold rich basalts. However, as noted by White and Hedenquist (1990), continental tholeiites similar to those of the bimodal assemblage generally are not prospects for epithermal gold-silver deposits.

The magmatic oxidation state and water content of magmas significantly influence the types and compositions of fluids released during cooling, crystallization, and degassing of magmas (e.g., Burnham and Ohmoto, 1980; Candela, 1997; Heinrich et al., 1999), and the absence of porphyry copper-gold and high-sulfidation gold deposits in the bimodal basalt-rhyolite assemblage probably is the direct result of the reduced and water-poor nature of magmas in this assemblage. Heinrich et al. (1999) showed that Au, Cu, As, and Sb are strongly partitioned into the vapor phase during vapor and liquid phase separation in high-temperature saline fluid systems but that oxidation state strongly affects metal partitioning. In reduced magmas, Cu and Au are much more strongly partitioned into the vapor phase, probably due to complexing by HS^-, than in oxidized magmas where sulfur is present mostly as SO_2 (Fig. 8; Whitney, 1984, 1988). Silver and other base metals (Pb, Zn) that are complexed by Cl^- are strongly partitioned into the saline brine.

In the oxidized, water-rich magmas of the western andesite assemblage, early saturation of the magma resulted in exsolution of a Cl- and S-rich aqueous fluid (Burnham, 1979). Partitioning of Au and Cu into the vapor relative to the brine was not as strong as in the more reduced bimodal assemblage magmas (Heinrich et al., 1999). The resulting brine may cool and form porphyry Cu-Au mineralization in and adjacent to the crystallizing magma (Fig. 13a). The vapor phase may separate and rise as an SO_2-rich plume that may mix with ground water, cool, and react with surrounding wall rocks to form extensive areas of propylitic alteration (the "primary neutralization" of Giggenbach, 1997; Fig. 13a) or it may react directly with volcanic wall rocks forming areas of advanced argillic alteration and acid-leaching characteristic of the upper parts of porphyry copper systems and early alteration in high-sulfidation deposits. Injection of unseparated, low- to moderate-salinity (ca. 5–10 wt % NaCl equiv), metal-rich, oxidized magmatic fluids into ground water during the late stages of magma crystallization may lead to the formation of relatively base metal and silver-rich low-sulfidation deposits in more distal parts of the hydrothermal system and high-sulfidation deposits in the advanced argillically altered rocks (Fig. 13a; Hedenquist and Lowenstern, 1994; Shinohara and Hedenquist, 1997; Hedenquist et al., 1998).

In reduced, water-poor magmas of the bimodal assemblage, sulfur is present primarily as H_2S, and the magmas may become saturated with an immiscible sulfide melt relatively early during their crystallization (Whitney, 1984, 1988; Candela, 1997). Copper will tend to partition into this sulfide phase. The low water contents of these magmas result in late fluid saturation that limits partitioning of compatible magmatic elements such as Cu into a magmatic aqueous vapor phase (Candela, 1997). Late vapor saturation of these magmas also results in a vapor rich in Au, As, and Sb (Heinrich et al., 1999), but the sulfur fugacity will be low due to buffering by pyrrhotite and magnetite (Whitney, 1984, 1988). Gold may be transported as a bisulfide complex in the vapor (Heinrich et al., 1999) and subsequently absorbed by meteoric water to generate the fluids that form low-sulfidation deposits with low Ag/Au ratios and high As, Hg, and Sb. In the extensional tectonic environment in which this assemblage formed where basalts were able to rapidly ascend from the upper mantle, hydrothermal fluids also may have risen rapidly from depth along deep open faults, as suggested by colloidal transport of electrum in many of the low-sulfidation deposits (Saunders et al., 1996).

Alternatively, the role of magmas in forming low-sulfidation deposits in the bimodal assemblage may have been little more than acting as a heat source to drive convective meteoric-hydrothermal systems. The geochemical signature for the low-sulfidation deposits (Au, Ag, As, Hg, Sb, Se, Tl) is similar to that for Carlin-type deposits (e.g., Arehart, 1996; Hofstra and Cline, 2000) with several notable exceptions (John and Wallace, 2000): in low-sulfidation deposits Ag contents are higher than in Carlin-type deposits, and the low-sulfidation deposits exhibit significant potassium metasomatism. Also, ore fluids in low-sulfidation deposits generally have much lower gas contents, probably due to the loss of CO_2, H_2S and other gases during boiling. Extensive decarbonation and argillic alteration of host rocks in Carlin-type deposits indicate moderately acidic fluids not in equilibrium with adularia. Most Carlin-type deposits are thought to have formed by cooling of deeply circulating meteoric and/or metamorphic water that scavenged metals, sulfur, and carbon from basement rocks (e.g., Hofstra and Cline, 2000), and low-sulfidation deposits

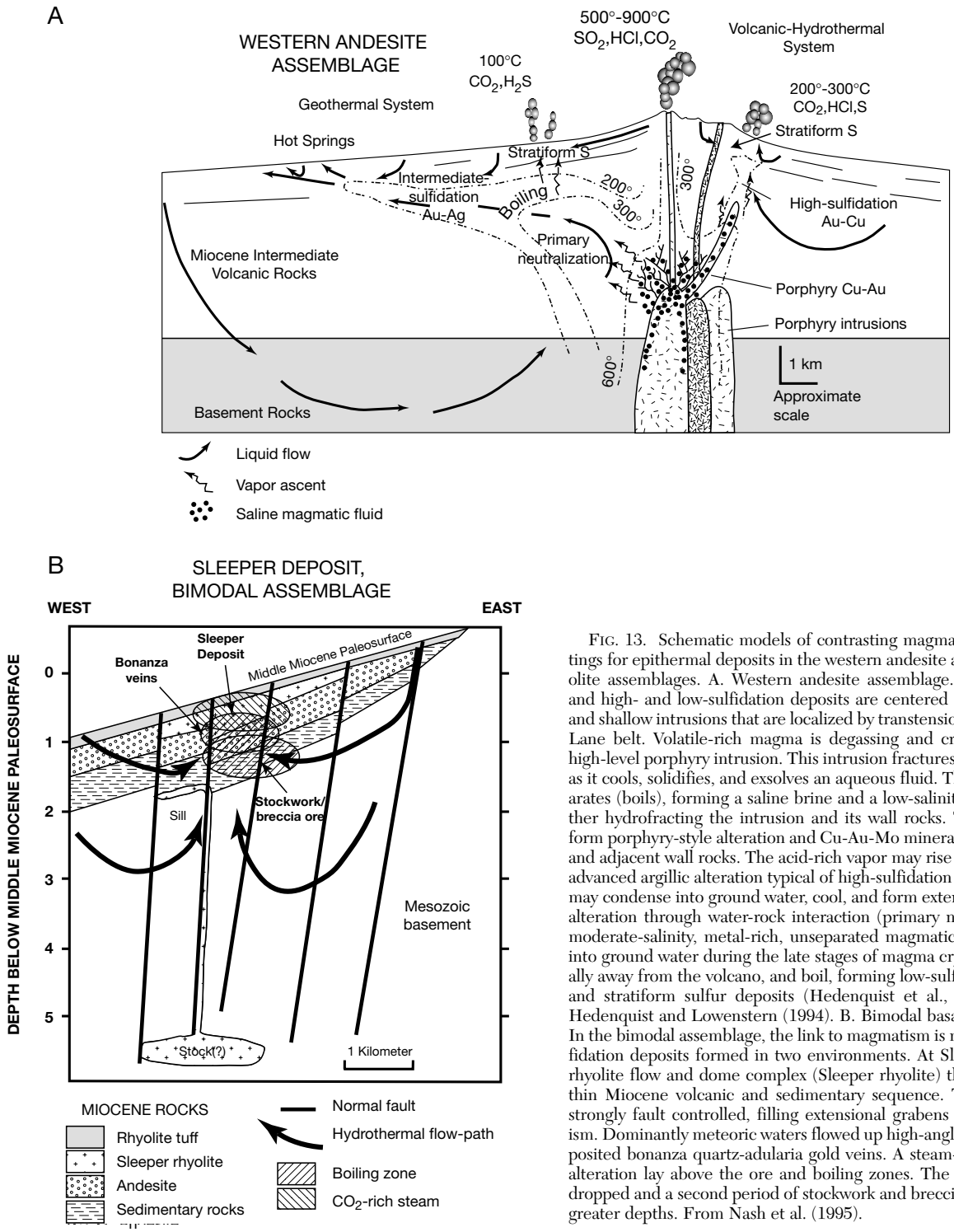

FIG. 13. Schematic models of contrasting magmatic and/or tectonic settings for epithermal deposits in the western andesite and bimodal basalt-rhyolite assemblages. A. Western andesite assemblage. Porphyry copper-gold and high- and low-sulfidation deposits are centered around stratovolcanoes and shallow intrusions that are localized by transtensional faults in the Walker Lane belt. Volatile-rich magma is degassing and crystallizing inward as a high-level porphyry intrusion. This intrusion fractures its wall rocks and itself as it cools, solidifies, and exsolves an aqueous fluid. This magmatic fluid separates (boils), forming a saline brine and a low-salinity acidic vapor and further hydrofracting the intrusion and its wall rocks. The brine may cool to form porphyry-style alteration and Cu-Au-Mo mineralization in the intrusion and adjacent wall rocks. The acid-rich vapor may rise and condense, forming advanced argillic alteration typical of high-sulfidation Au-Cu deposits. It also may condense into ground water, cool, and form extensive areas of propylitic alteration through water-rock interaction (primary neutralization). Low- to moderate-salinity, metal-rich, unseparated magmatic fluid may be injected into ground water during the late stages of magma crystallization, flow laterally away from the volcano, and boil, forming low-sulfidation Au-Ag deposits and stratiform sulfur deposits (Hedenquist et al., 1998). Modified from Hedenquist and Lowenstern (1994). B. Bimodal basalt-rhyolite assemblage. In the bimodal assemblage, the link to magmatism is more tenuous. Low-sulfidation deposits formed in two environments. At Sleeper, host rocks are a rhyolite flow and dome complex (Sleeper rhyolite) that overlies a relatively thin Miocene volcanic and sedimentary sequence. The volcanic rocks are strongly fault controlled, filling extensional grabens formed during volcanism. Dominantly meteoric waters flowed up high-angle faults, boiled, and deposited bonanza quartz-adularia gold veins. A steam-heated zone of argillic alteration lay above the ore and boiling zones. The water table apparently dropped and a second period of stockwork and breccia ore formed at slightly greater depths. From Nash et al. (1995).

could be shallow-level manifestations of similar hydrothermal systems driven by magmatic heat sources.

Classification of epithermal deposits and use of the term intermediate-sulfidation deposits

Hedenquist et al. (2000) proposed the subdivision of low-sulfidation deposits into two groups, intermediate-sulfidation and end-member low-sulfidation, based on inferred variations in the sulfidation state of ore assemblages. They noted that this subdivision was not simply a distinction in sulfide mineral assemblages, but rather an attempt to "recognize and distinguish the possibility that intermediate-sulfidation deposits form in different tectonic settings and have different magmatic affiliations" (p. 250). They also noted that their proposed subdivision was based in part on characteristics of low-sulfidation deposits in the northern Great Basin (John, 1999; John et al., 1999).

The usefulness of a classification system for deposit types is dependent on identification of characteristics that allow clear separation of deposits into distinct groups. In general, Miocene and early Pliocene low-sulfidation deposits in the northern Great Basin clearly separate into two groups as outlined in Tables 4 and 6. These two groups of deposits generally are spatially and temporally associated with different compositions and styles of magmatism, formed in different tectonic settings, contain consistent mineralogical differences, and have different Au/Ag ratios. However, the sulfidation and oxidation states of most deposits have not been rigorously evaluated, and the genetic relationship of most low-sulfidation deposits in the bimodal assemblage to magmatism remains unresolved. In addition, there are several exceptions to these generalized groupings; deposits in the Aurora and Rawhide districts in the western andesite assemblage that contain minor amounts of selenide minerals and have low base metal contents and reduced sulfide mineral assemblages relative to other intermediate-sulfidation deposits in the western andesite assemblage, and deposits in the Delamar district in the bimodal assemblage that have anomalously high Ag/Au ratios relative to other end-member low-sulfidation deposits. Deposits in the Aurora and Rawhide districts are spatially and temporally associated with rhyolite dome complexes, similar to low-sulfidation deposits in the bimodal assemblage and atypical of most other epithermal deposits in the western andesite assemblage. Deposits in the Delamar district that lie north of the Great Basin along the Snake River plain may overlie lower crustal rocks different from other deposits in the Great Basin and may have formed from ore fluids with higher salinities than other low-sulfidation deposits in the bimodal assemblage.

If the classification system for epithermal deposits proposed by Hedenquist et al. (2000) is to be widely adopted, detailed studies of deposits in other regions that formed in variable tectonic settings from variable styles of magmatism should be conducted to see if there are consistent relationships between deposit characteristics, magmatism, and tectonic setting, as discussed above. A more rigorous evaluation of the sulfidation and oxidation states of ore-forming fluids in well characterized deposits also should be undertaken to see if there are consistent variations in the sulfidation and oxidation state that correlate with other deposit characteristics and justify separation of intermediate-sulfidation deposits from other low-sulfidation deposits.

Conclusions and Implications for Exploration

Many major epithermal gold-silver deposits, including the world-class Comstock Lode, Tonopah, Goldfield, and Ken Snyder (Midas), formed during the Miocene and early Pliocene in the northern Great Basin. These deposits are closely associated spatially and temporally with two magmatic assemblages—western andesite and bimodal basalt-rhyolite—that were widespread across the Great Basin. The types and characteristics of epithermal deposits vary systemically with these magmatic assemblages. These variations largely reflect differences in the tectonic environment in which the magmas were generated and emplaced and may reflect variable magmatic contributions to ore-forming fluids. However, the magmatic input, if any, to ore-forming fluids for most low-sulfidation deposits in the bimodal assemblage remains ambiguous.

The distribution and characteristics of Miocene and early Pliocene magmatism and epithermal deposits in the northern Great Basin have important implications for exploration both there and in other areas with similar tectonic-magmatic settings:

1. Porphyry Cu-Au and high-sulfidation Au-Ag deposits are found only in the western andesite assemblage. Their formation is favored by the shallow intrusion of moderate to large bodies of oxidized calc-alkaline magma with high water content that is characteristic of this assemblage. These deposits are absent in the continental rift-related bimodal basalt-rhyolite assemblage.
2. Recent structural analyses of several epithermal deposits in the western andesite assemblage suggest that many deposits are localized in releasing bends and stepovers in transtensional zones related to strike-slip faults. These structures may have guided emplacement of both magmas and mineral deposits and may be useful exploration guides within local areas.
3. Low-sulfidation deposits in the western andesite assemblage formed peripherally to high-sulfidation gold deposits and suspected porphyry Cu-Au systems. These deposits formed throughout the life of the western andesite assemblage (22–4 Ma) and are themselves small parts of much larger hydrothermal systems that may be largely concealed beneath younger, unmineralized rocks. These deposits generally have higher Ag/Au ratios and base metal contents than low-sulfidation deposits in the bimodal assemblage.
4. Low-sulfidation deposits in the bimodal assemblage, typically of a bonanza vein character, formed primarily in a narrow (16–14 Ma) time window during the early stages of the Basin and Range extension. These deposits and their alteration products are controlled closely by faults related to this extension and did not develop large areas of propylitic alteration. This small footprint means that they are easily covered by younger, unmineralized rocks, thus making exploration for these narrow vein deposits difficult.

Acknowledgments

Discussions with Alan Wallace, Barney Berger, Jeff Hedenquist, Stuart Simmons, Larry Garside, Hal Bonham, Chris Henry, Jim Rytuba, Steve Ludington, Peter Vikre, Marco Einaudi, Eric Saderholm, Dick Tosdal, and Al Hofstra are gratefully acknowledged. Chris Henry and Roger Ashley provided unpublished data. Jeff Hedenquist, Steve Ludington, Ted Theodore, Peter Vikre, Alan Wallace, Eric Seedorff, Stuart Simmons, Noel White, and Barney Berger provided helpful comments on earlier versions of this paper.

January 30, July 18, 2001

REFERENCES

Albino, G.V., 1991, Washington Hill prospect: Association of Exploration Geochemists International Geochemical Exploration Symposium, 15th, Reno, Nevada, April 25–28, 1991, Field Trip 16, p. 193–198.

Albino, G.V., and Boyer, C., 1992, Lithologic and structural control of gold deposits of the Santa Fe district, Mineral County, Nevada: Walker Lane Symposium, Reno, April 24, 1992, Proceedings Volume, p. 187–211.

Albino, G.V., and Margolis, J., 1991, Differing styles of adularia-sericite

epithermal deposits—contrasts in geologic setting and mineralogy [abs.]: Geological Society of America Abstracts with Programs, v. 23, p. A230.
Andersen, D.P., Bishop, F.C., and Lindsley, D.H., 1991, Internally consistent solution models for Fe-Mg-Mn-Ti oxides: Part II. Fe-Mg-Ti oxides and olivine: American Mineralogist, v. 76, p. 427–444.
Arehart, G.B, 1996, Characteristics and origin of sediment-hosted disseminated gold deposits: A review: Ore Geology Reviews, v. 11, p. 383–403.
Arribas, A., Jr., 1995, Characteristics of high-sulfidation epithermal deposits, and their relation to magmatic fluid: Mineralogical Association of Canada Short Course Series, v. 23, p. 419–454.
Ashley, R.P., 1974, Goldfield mining district: Nevada Bureau of Mines and Geology Report 19, p. 49–66.
——1979, Relation between volcanism and ore deposition at Goldfield, Nevada: Nevada Bureau of Mines and Geology Report 33, p. 77–86.
——1990, The Goldfield gold district, Esmeralda and Nye Counties, Nevada: U.S. Geological Survey Bulletin 1857-H, p. H1–H7.
Ashley, R.P., and Silberman, M.L., 1976, Direct dating of mineralization at Goldfield, Nevada, by potassium-argon and fission-track methods: Economic Geology, v. 71, p. 904–924.
Atwater, T., 1970, Implications of plate tectonics for the Cenozoic tectonic evolution of western North America: Geological Society of America Bulletin, v. 81, p. 3513–3535.
Axen, G.J., Taylor, W.J., and Bartley, J.M., 1993, Space-time patterns and tectonic controls of Tertiary extension and magmatism in the Great Basin of the western United States: Geological Society of America Bulletin, v. 105, p. 56–76.
Babcock, R.C., Jr., Ballantyne, G.H., and Phillips, C.H., 1995, Summary of the geology of the Bingham district, Utah: Utah Geological Society Digest, v. 20, p. 316–335.
Bacon, C.R., and Hirschmann, M.M., 1988, Mg/Mn partitioning as a test for equilibrium between co-existing Fe-Ti oxides: American Mineralogist, v. 73, p. 57–61.
Barton, P.B., and Skinner, B.J., 1979, Sulfide mineral stabilities, *in* Barnes, H.L., ed., Geochemistry of hydrothermal ore deposits, 2nd ed.: New York, Wiley Interscience, p. 278–403.
Berger, B.R., 1996, Constraining structural environments during fault motion inversion; requisite for bonanza orebody formation, Comstock Lode, Virginia City, Nevada [abs.]: Geological Society of America Abstracts with Programs, v. 28, no. 7, p. 94.
Berger, B.R., and Drew, L.J., 1997, Role of strike-slip duplexes in localization of volcanoes, related intrusions, and epizonal ore deposits [abs.]: Geological Society of America Abstracts with Programs, v. 29, no. 6, p. 359–360.
Berger, B.R., Snee, L.W., and Tingley, J.V., 1999, Implications of new structural and $^{40}Ar/^{39}Ar$ data on hydraulic evolution of epithermal veins and ore formation, Aurora and Bodie mining districts, Nevada-California [abs.]: Geological Society of America Abstracts with Programs, v. 31, no. 7, p. A94.
Best, M.G., Christiansen, E.H., Deino, A.L., Grommé, C.S., McKee, E.H., and Noble, D.C., 1989, Excursion 3A: Eocene through Miocene volcanism in the Great Basin of the western United States: New Mexico Bureau of Mines and Mineral Resources Memoir 47, p. 91–133.
Black, J.E., Mancuso, T.K., and Gant, J.L., 1991, Geology and mineralization at the Rawhide Au-Ag deposit, Mineral County, Nevada, *in* Raines, G.L., Lisle, R.E., Schafer, R.W., and Wilkinson, W.H., eds., Geology and ore deposits of the Great Basin. Symposium proceedings: Reno, Geological Society of Nevada and U.S. Geological Survey, p. 1123–1144.
Blair, K.R., 1991, Geology of the Gold Circle district, Elko County, Nevada: Unpublished M.Sc. thesis, Tucson, University of Arizona, 85 p.
Blakely R.J., and Jachens, R.C., 1991, Regional study of mineral resources in Nevada—insights from three-dimensional analysis of gravity and magnetic anomalies: Geological Society of America Bulletin, v. 103, p. 795–803.
Bonham, H.F., Jr., 1969, Geology and mineral deposits of Washoe and Storey Counties, Nevada, with a section on industrial rock and mineral deposits by K. L. Papke: Nevada Bureau of Mines and Geology Bulletin 70, 140 p.
Bonham, H.F., Jr., and Garside, L.J., 1979, Geology of the Tonopah, Lone Mountain, Klondike, and northern Mud Spring Lake quadrangles, Nevada: Nevada Bureau of Mines and Geology Bulletin 92, 136 p.
Breit, F.J., Jr., Silberman, M.L., Noble, D.C., Hardyman, R.F., Snee, L.W., and Percival, T.J., 1995, Structural and temporal relationships and geochemical characteristics of the East Brawley Peak acid-sulfate and adjacent Aurora adularia-sericite systems [abs.]: Geological Society of Nevada, Geology and Ore Deposits of the American Cordillera Symposium, April 10–13, 1995, Reno, Nevada, Abstracts, p. A14.
Brooks, W.E., Thorman, C.H., and Snee, L.W., 1995, The $^{40}Ar/^{39}Ar$ ages and tectonic setting of the middle Eocene northeast Nevada volcanic field: Journal of Geophysical Research, v. 100, p. 10,403–10,416.
Browne, P.R.L., and Lovering, J.F., 1973, Composition of sphalerites from the Broadlands geothermal field and their significance to sphalerite geothermometry and geobarometry: Economic Geology, v. 68, p. 381–387.
Burchfiel, B.C., Cowan, D.S., and Davis, G.A., 1992, Tectonic overview of the Cordilleran orogeny in the western United States: Geological Society of America, Geology of North America, v. G-3, p. 407–479.
Burnham, C.W., 1979, Magmas and hydrothermal fluids, *in* Barnes, H.L., ed., Geochemistry of hydrothermal ore deposits, 2nd ed.: New York, Wiley Interscience, p. 71–136.
Burnham, C.W., and Ohmoto, H., 1980, Late stage processes of felsic magmatism: Society of Mining Geology of Japan Special Issue 8, p. 1–11.
Bussey, S.D., 1996, Gold mineralization and associated rhyolitic volcanism at the Hog Ranch district, northwest Nevada: Geological Society of Nevada, Geology and Ore Deposits of the American Cordillera Symposium, Reno-Sparks, Nevada, April 1995, Proceedings, p. 181–207.
Canby, V.M., 1992, Porphyry-type gold mineralization of late Neogene age at the Zule volcanic center, Sierra County, California: Unpublished M.Sc., thesis, Reno, University of Nevada, 108 p.
Candela, P.A., 1997, A review of shallow, ore-related granites: Textures, volatiles, and ore metals: Journal of Petrology, v. 38, p. 1619–1633.
Carlson, R.W., and Hart, W.K., 1987, Crustal genesis on the Oregon plateau: Journal of Geophysical Research, v. 92, p. 6191–6206.
Carmichael, I.S.E., 1967, The iron-titanium oxides of salic volcanic rocks and their associated ferromagnesium silicates: Contributions to Mineralogy and Petrology, v. 14, p. 36–64.
Chesterman, C.W., and Gray, C.H., Jr., 1975, Geology of the Bodie quadrangle, Mono County, California: California Division of Mines and Geology Map Sheet 21, scale: 1:48,000.
Chesterman, C.W., Chapman, R.H., and Gray, C.H., Jr., 1986, Geology and ore deposits of the Bodie mining district, Mono County, California: California Division of Mines and Geology Report 206, 36 p.
Christiansen, R.L., and Lipman, P.W., 1972, Cenozoic volcanism and plate tectonic evolution of the western United States. II. Late Cenozoic: Philosophical Transactions of the Royal Society of London, Series A, v. 271, p. 249–284.
Christiansen, R.L., and Yeats, R.S., 1992, Post-Laramide geology of the U.S. Cordilleran region: Geological Society of America, Geology of North America, v. G-3, p. 261–406.
Coats, R.R., 1940, Propylitization and related types of alteration on the Comstock Lode: Economic Geology, v. 35, p. 1–16.
Connors, K.A., Noble, D.C., Bussey, S.D., and Weiss, S.I., 1993, Initial gold contents of silicic volcanic rocks: Bearing on the behavior of gold in magmatic systems: Geology, v. 21, p. 937–940.
Conrad, J.E., and McKee, E.H., 1996, High-precision $^{40}Ar/^{39}Ar$ ages of rhyolitic host rock and mineralized veins at the Sleeper deposit, Humboldt County, Nevada: Geological Society of Nevada, Geology and Ore Deposits of the American Cordillera Symposium, Reno-Sparks, Nevada, April 1995, Proceedings, p. 257–262.
Conrad, J.E., McKee, E.H., Rytuba, J.J., Nash, J.T., and Utterback, W.C., 1993, Geochronology of the Sleeper deposit, Humboldt County, Nevada: Epithermal gold-silver mineralization following emplacement of a silicic flow-dome complex: Economic Geology, v. 88, p. 81–91.
Conrad, W.K., 1984, The mineralogy and petrology of compositionally zoned ash flow tuffs, and related silicic rocks, from the McDermitt caldera complex, Nevada-Oregon: Journal of Geophysical Research, v. 89, p. 8639–8664.
Cooke, D.R., and Simmons, S.F., 2000, Characteristics and genesis of epithermal gold deposits: Reviews in Economic Geology, v. 13, p. 221–244.
Davidson, J.P., and de Silva, S.L., 1995, Late Cenozoic magmatism of the Bolivian Altiplano: Contributions to Mineralogy and Petrology, v. 11, p. 387–408.
Derkey, R.E., Joeseph, N.L., and Lasmanis, R., 1990, Metal mines of Washington: Preliminary report: Washington Division of Geology and Earth Resources Open-File Report 90-18, 577 p.
Dilles, J.H., and Gans, P.B., 1995, The chronology of Cenozoic volcanism and deformation in the Yerington area, western Basin and Range and Walker Lane: Geological Society of America Bulletin, v. 107, p. 474–486.
Ebert, S.W., Groves, D.I., and Jones, J.K., 1996, Geology, alteration, and ore controls of the Crofoot/Lewis mine, Sulphur, Nevada: Geological Society of Nevada, Geology and Ore Deposits of the American Cordillera Symposium, Reno-Sparks, Nevada, April 1995, Proceedings, p. 209–234.

Ekren, E.B., and Byers, F.M., Jr., 1984, The Gabbs Valley Range—a well exposed segment of the Walker Lane in west-central Nevada, *in* Lintz, J., Jr., ed., Western geologic excursions: Geological Society of America, Annual Meeting, Reno, Nevada, Guidebook, v. 4, p. 203–215.

Ekren, E.B., Byers, F.M., Jr., Hardyman, R.F., Marvin, R.F., and Silberman, M.L., 1980, Stratigraphy, preliminary petrology, and some structural features of Tertiary volcanic rocks in the Gabbs Valley and Gillis Ranges, Nevada: U.S. Geological Survey Bulletin 1464, 54 p.

Eng, T., 1991, Geology and mineralization of the Freedom Flats gold deposit, Borealis mine, Mineral County, Nevada, *in* Raines, G.L., Lisle, R.E., Schafer, R.W., and Wilkinson, W.H., eds., Geology and ore deposits of the Great Basin. Symposium proceedings: Reno, Geological Society of Nevada and U.S. Geological Survey, p. 995–1019.

Eng, T., Boden, D.R., Reischman, M.R., and Biggs, J.O., 1996, Geology and mineralization of the Bullfrog mine and vicinity, Nye County, Nevada: Geological Society of Nevada, Geology and Ore Deposits of the American Cordillera Symposium, Reno-Sparks, Nevada, April 1995, Proceedings, p. 353–402.

Evans, J.R., 1977, Zaca mine and Leviathan mine: California Division of Mines and Geology County Report 8, p. 22–27.

Fahley, M.P., 1979, Fluid inclusion study of the Tonopah district: Unpublished M.Sc. thesis, Golden, Colorado School of Mines, 106 p.

Feeley, T.C., and Grunder, A.L., 1991, Mantle contribution to the evolution of middle Tertiary silicic magmatism during early stages of extension: the Egan Range volcanic complex, east-central Nevada: Contributions to Mineralogy and Petrology, v. 106, p. 154–169.

Fiannaca, M., 1987, Geology of the Santa Fe gold-silver deposit, Mineral County, Nevada, *in* Johnson, J.L., ed., Bulk mineable precious metal deposits of the western United States: Reno, Geological Society of Nevada, p. 233–239.

Fitton, J.G., James, D., and Leeman, W.P., 1991, Basic magmatism associated with late Cenozoic extension in the western United States: Compositional variations in space and time: Journal of Geophysical Research, v. 96, p. 13,693–13,711.

Fries, C., 1942, Tin deposits of northern Lander County, Nevada: U.S. Geological Survey Bulletin 931-L, p. 279–294.

Gans, P.B., 1987, An open-system, two-layer crustal stretching model for the eastern Great Basin: Tectonics, v. 6, p. 1–12.

Gans, P.B., and Bohrson, W.A., 1998, Suppression of volcanism during rapid extension in the Basin and Range province, United States: Science, v. 279, p. 66–68.

Gans, P.B., Mahood, G.A., and Schermer, E., 1989, Synextensional magmatism in the Basin and Range province: A case study from the eastern Great Basin: Geological Society of America Special Paper 233, 53 p.

Giggenbach, W.F., 1992a, Magma degassing and mineral deposition in hydrothermal systems along convergent plate boundaries: ECONOMIC GEOLOGY, v. 87, p. 1927–1944.

——1992b, The composition of gases in geothermal and volcanic systems as a function of tectonic setting: International Symposium on Water-Rock Interaction, 7th, Park City, Utah, Proceedings, p. 873–878.

——1992c, Isotopic shifts in waters from geothermal and volcanic systems along convergent plate boundaries and their origins: Earth and Planetary Science Letters, v. 113, p. 495–510.

——1995, Variations in the chemical and isotopic composition of fluids discharged from the Taupo Volcanic Zone, New Zealand: Journal of Volcanology and Geothermal Research, v. 68, p. 89–116.

——1997, The origin and evolution of fluids in magmatic-hydrothermal systems, *in* Barnes, H. L., ed., Geochemistry of hydrothermal ore deposits, 3rd ed.: New York, John Wiley and Sons, p. 737–796.

Gill, J.B., 1981, Orogenic andesites and plate tectonics: Berlin, Springer-Verlag, 390 p.

Goldstrand, P.M., and Schmidt, K.W., 2000, Geology, mineralization, and ore controls at the Ken Snyder gold-silver mine, Elko County, Nevada: Geological Society of Nevada, Geology and Ore Deposits 2000: The Great Basin and Beyond Symposium, May 15–18, 2000, Reno-Sparks, Nevada, Proceedings, p. 265–287.

Graham, I.J., Cole, J.W., Briggs, R.M., Gamble, J.A., and Smith, I.E.M., 1995, Petrology and petrogenesis of volcanic rocks from the Taupo Volcanic Zone: A review: Journal of Volcanology and Geothermal Research, v. 68, p. 59–87.

Graney, J.R., and Kesler, S.E., 1995, Gas composition of inclusion fluid in ore deposits: Is there a relation to magmas?: Mineralogical Association of Canada Short Course Series, v. 23, p. 221–245.

Gray, D.S., 1996, Structural controls of precious metal mineralization at the Denton-Rawhide mine, Rawhide, Nevada: Geological Society of Nevada, Geology and Ore Deposits of the American Cordillera Symposium, Reno-Sparks, Nevada, April 1995, Proceedings, p. 263–281.

Grose, T.L.T., 2000, Volcanoes in the Susanville region, Lassen, Modoc, Plumas Counties, northeastern California: California Geology, v. 53, no. 5, p. 4–24.

Halsor, S.P., Bornhorst, T.J., Beebe, M., Richardson, K., and Strowd, W, 1988, Geology of the DeLamar silver mine, Idaho—a volcanic dome complex and genetically associated hydrothermal system: ECONOMIC GEOLOGY, v. 83, p. 1159–1169.

Haney, J.P., Steffen, J.B., Starr, J.B., Payne, J.D., McCelland, W.C., and Oldow, J.S., 2000, Structural controls on epithermal mineralization in the Borealis district, Nevada [abs.]: Geological Society of America Abstracts with Programs, v. 32, no. 7, p. 82.

Hardyman, R.F., and Oldow, J.S., 1991, Tertiary tectonic framework and Cenozoic history of the central Walker Lane, Nevada, *in* Raines, G.L., Lisle, R.E., Schafer, R.W., and Wilkinson, W.H., eds., Geology and ore deposits of the Great Basin. Symposium proceedings: Reno, Geological Society of Nevada and U.S. Geological Survey, p. 279–302.

Harvey, D.S., Noble, D.C., and McKee, E.H., 1986, Hog Ranch gold property, northwestern Nevada: Age and genetic relation of hydrothermal mineralization to coeval peralkaline silicic and associated basaltic magmatism: Isochron/West, no. 47, p. 9–11.

Heald, P., Foley, N.K., and Hayba, D.O., 1987, Comparative anatomy of volcanic-hosted epithermal deposits: Acid sulfate and adularia-sericite types: ECONOMIC GEOLOGY, v. 82, p. 1–26.

Hedenquist, J.W., and Henley, R.W., 1985, The importance of CO_2 on freezing point measurements of fluid inclusions: Evidence from active geothermal systems and implications for epithermal ore deposition: ECONOMIC GEOLOGY, v. 80, p. 1379–1406.

Hedenquist, J.W., and Lowenstern, J.B., 1994, The role of magmas in the formation of hydrothermal ore deposits: Nature, v. 370, p. 519–527.

Hedenquist, J.W., Arribas, A., Jr., and Reynolds, T.J., 1998, Evolution of an intrusion-centered hydrothermal system: Far Southeast–Lepanto porphyry and epithermal Cu-Au deposits, Philippines: ECONOMIC GEOLOGY, v. 93, p. 373–404.

Hedenquist, J.W., Arribas, A., Jr., and Gonzalez-Urien, E., 2000, Exploration for epithermal gold deposits: Reviews in Economic Geology, v. 13, p. 245–277.

Heinrich, C.A., Gunther, D., Audetat, A., Ulrich, T., and Frischknecht, R., 1999, Metal fractionation between magmatic brine and vapor, determined by microanalysis of fluid inclusions: Geology, v. 27, p. 755–758.

Henley, R.W., 1990, Ore transport and deposition in epithermal environments: University of Western Australia Geology Department Publication 23, p. 51–69.

Henley, R.W., and Ellis, A.J., 1983, Geothermal systems ancient and modern: A geochemical review: Earth-Science Reviews, v. 19, p. 1–50.

Henry, C.D., 1996, Geologic map of the Bell Mountain quadrangle, western Nevada: Nevada Bureau of Mines and Geology Field Studies Map 12, scale 1:24,000, 14 p.

Henry, C.D., and Ressel, M.W., 2000, Interrelation of Eocene magmatism, extension, and Carlin-type gold deposits in northeastern Nevada: Geological Society of America Field Guide 2, p. 165–187.

Hildreth, E.W., 1981, Gradients in silicic magma chambers: Implications for lithospheric magmatism: Journal of Geophysical Research, v. 86, p. 10,153–10,192.

Hildreth, E.W., and Moorbath, S., 1988, Crustal contributions to arc magmatism in the Andes of central Chile: Contributions to Mineralogy and Petrology, v. 98, p. 455–489.

Hofstra, A.H., and Cline, J.S., 2000, Characteristics and models for Carlin-type gold deposits: Reviews in Economic Geology, v. 13, p. 163–220.

Hollister, V.F., and Silberman, M.L., 1995, Silver-gold and polymetallic quartz veins in the Bodie mining district, east-central California—are they related to a porphyry Cu-Mo system at depth?: Arizona Geological Society Digest, v. 20, p. 297–305.

Honjo, N., Bonnichsen, B., Leeman, W.P., and Stormer, J.C., Jr., 1992, Mineralogy and geothermometry of high-temperature rhyolites from the central and western Snake River plain: Bulletin of Volcanology, v. 54, p. 220–237.

Hooper, P.R., and Hawkesworth, C.J., 1993, Isotopic and geochemical constraints on the origin and evolution of the Columbia River basalt: Journal of Petrology, v. 34, p. 1203–1246.

Hudson, D.M., 1977, Geology and alteration of the Wedekind and part of the Peavine districts, Washoe County, Nevada: Unpublished M.Sc. thesis, Reno, University of Nevada, 102 p

——1983, Alteration and geochemical characteristics of the upper parts of selected porphyry systems, western Nevada: Unpublished Ph.D. dissertation, Reno, University of Nevada, 229 p.

——1993, The Comstock district, *in* Lahren, M.M. Trexler, J.H., Jr., and Spinoza, C., eds., Crustal evolution of the Great Basin and Sierra Nevada: Geological Society of America, Cordilleran-Rocky Mountain sections, Guidebook, p. 481–496.

Humphreys, E.D., 1995, Post-Laramide removal of the Farallon slab, western United States: Geology, v. 23, p. 987–990.

Ioannou, S.E., and Spooner, E.T.C., 2000, Miocene epithermal Au-Ag characteristics and controls; Dixie claims, Midas district, north-central Nevada [abs.]: Geological Society of America Abstracts with Program, v. 31, no. 7, p. A-83.

Irvine, T.N., and Baragar, W.R.A., 1971, A guide to the chemical classification of the common volcanic rocks: Canadian Journal of Earth Sciences, v. 8, p. 523–548.

John, D.A., 1992, Stratigraphy, regional distribution, and reconnaissance geochemistry of Oligocene and Miocene volcanic rocks in the Paradise Range and northern Pactolus Hills, Nye County, Nevada: U.S. Geological Survey Bulletin 1974, 67 p.

——1999, Magmatic influence on characteristics of Miocene low-sulfidation Au-Ag deposits in the northern Great Basin [abs.]: Geological Society of America Abstracts with Program, v. 31, no. 7, p. A-405.

——2000, Magmas and Miocene low-sulfidation Au-Ag deposits in the northern Great Basin [abs.]: Geological Society of America Abstracts with Program, v. 31, no. 7, p. A-250.

John, D.A., and Wallace, A.R., 2000, Epithermal gold-silver mineral deposits related to the northern Nevada rift: Geological Society of Nevada, Geology and Ore Deposits 2000: The Great Basin and Beyond Symposium, May 15–18, 2000, Reno-Sparks, Nevada, Proceedings, p. 155–175.

John, D.A., Thomason, R.E., and McKee, E.H., 1989, Geology and K-Ar geochronology of the Paradise Peak mine and the relationship of pre-Basin and Range extension to early Miocene precious metal mineralization in west-central Nevada: ECONOMIC GEOLOGY, v. 84, p. 631–649.

John, D.A., Nash, J.T., Clark, C.W., and Wulftange, W., 1991, Geology, hydrothermal alteration, and mineralization at the Paradise Peak gold-silver-mercury deposit, Nye County, Nevada, *in* Raines, G.L., Lisle, R.E., Schafer, R.W., and Wilkinson, W.H., eds., Geology and ore deposits of the Great Basin. Symposium proceedings: Reno, Geological Society of Nevada and U.S. Geological Survey, p. 1020–1050.

John, D.A., Garside, L.J., and Wallace, A.R., 1999, Magmatic and tectonic setting of late Cenozoic epithermal gold-silver deposits in northern Nevada, with an emphasis on the Pah Rah and Virginia Ranges and the northern Nevada rift: Geological Society of Nevada, 1999 Spring Field Trip Guidebook Special Publication 29, p. 64–158.

John, D.A., Wallace, A.R., Ponce, D.A., Fleck, R., and Conrad, J.E., 2000, New perspectives on the geology and origin of the northern Nevada rift: Geological Society of Nevada, Geology and Ore Deposits 2000: The Great Basin and Beyond Symposium, May 15–18, 2000, Reno-Sparks, Nevada, Proceedings, p. 127–154.

Johnson, J.A., and Grunder, A.L., 2000, The making of intermediate composition magma in a bimodal suite: Duck Butte eruptive center, Oregon, USA: Journal of Volcanology and Geothermal Research, v. 95, p. 175–195.

Karlstrom, K.E., Harlan, S.S., Williams, M.L., McLelland, J., Geissman, J.W., and Åhåll, K.-I., 1999, Refining Rodinia: Geologic evidence for the Australia-Western U.S. connection in the Proterozoic: Geological Society of America Today, v. 9, no. 10, p. 1–7.

Keith, J.D., and Shanks, W.C., III, 1988, Chemical evolution and volatile fugacities of the Pine Grove porphyry molybdenum and ash flow tuff system, southwestern Utah: Canadian Institute of Mining and Metallurgy Special Volume 39, p. 402–423.

Kistler, R.W., 1991, Chemical and isotopic characteristics of plutons in the Great Basin, *in* Raines, G.L., Lisle, R.E., Schafer, R.W., and Wilkinson, W.H., eds., Geology and ore deposits of the Great Basin. Symposium proceedings: Reno, Geological Society of Nevada and U.S. Geological Survey, p. 107–109.

Leavitt, E.D., Arehart, G.B., and Goldstrand, P.M., 2000a, Hydrothermal alteration associated with the Colorado Grande vein, Ken Snyder mine, Elko County, Nevada [abs.]: Geological Society of America Abstracts with Programs, v. 32, no. 7, p. 251.

Leavitt, E.D., Goldstrand, P., Schmidt, K., Wallace, A.R., Spell, T., and Arehart, G.B., 2000b, Geochronology of the Midas gold-silver deposit and its relationship to volcanism and mineralization along the northern Nevada rift: Geological Society of Nevada, Geology and Ore Deposits 2000: The Great Basin and Beyond Symposium, May 15–18, 2000, Reno-Sparks, Nevada, Field Trip Guidebook 8, p. 157–162.

Le Bas, M.J., LeMaitre, R.W., Streckeisen, A., and Zanettin, B., 1986, A chemical classification of volcanic rocks based on the total alkali-silica diagram: Journal of Petrology, v. 27, p. 745–750.

Lindgren, W., 1933, Mineral deposits, 4th ed.: New York, McGraw-Hill, 930 p.

Lipman, P.W., Protska, H.J., and Christiansen, R.L., 1972, Cenozoic volcanism and plate tectonic evolution of the western United States, I. Early and middle Cenozoic: Philosophical Transactions of the Royal Society of London, Series A, v. 271, p. 217–248.

Locke, A., Billingsley, P.R., and Mayo, E.B., 1940, Sierra Nevada tectonic patterns: Geological Society of America Bulletin, v. 51, p. 513–540.

Long, K.R., DeYoung, J.H., and Ludington, S.D., 1998, Database of significant deposits of gold, silver, copper, lead, and zinc in the United States; U.S. Geological Survey Open-File Report 98-0206-A, 33 p., 98-206B, one 3.5-inch diskette.

Ludington, S., McKee, E.H., Cox, D.P., Leonard, K.W., and Moring, B.C., 1996a, Pre-Tertiary geology of Nevada: Nevada Bureau of Mines and Geology Open-File Report 96-2, p. 4–1 to 4–9.

Ludington, S., Cox, D.P., Moring, B.C., and Leonard, K.W., 1996b, Cenozoic volcanic geology of Nevada: Nevada Bureau of Mines and Geology Open-File Report 96-2, p. 5–1 to 5–10.

Luhr, J.F., 1992, Slab-derived fluids and partial melting in subduction zones: Insights from two contrasting Mexican volcanoes (Colima and Ceboruco): Journal of Volcanology and Geothermal Research, v. 54, p. 1–18.

Mabey, D.R., 1966, Regional gravity and magnetic anomalies in part of Eureka County, Nevada, *in* Hansen, D.A., et al., eds., Mining geophysics: Tulsa, Oklahoma, Society of Exploration Geophysicists, v. 1, p. 77–83.

Margolis, J., 1993, Tectonic and magmatic controls on the metal composition of some Cenozoic hydrothermal systems of the northwestern U.S. [abs.]: Geological Society of America Abstracts with Programs, v. 25, no. 5, p. 114.

McKee, E.H., 1971, Tertiary igneous chronology of the Great Basin of the western United States—implications for tectonic models: Geological Society of America Bulletin, v. 82, p. 3497–3502.

McKee, E.H., and Klock, P.R., 1984, K-Ar ages of Cenozoic volcanic rocks, Walker Lake 1° X 2° quadrangle, eastern California and western Nevada: Isochron/West, no. 40, p. 9–11.

McKee, E.H., and Moring, B.C., 1996, Cenozoic mineral deposits and related rocks: Nevada Bureau of Mines and Geology Open-File Report 96–2, p. 6–1 to 6–8.

McKee, E.H., Noble, D.C., and Silberman, M.L., 1970, Middle Miocene hiatus in volcanic activity in the Great Basin area of the western United States: Earth and Planetary Science Letters, v. 8, p. 93–96.

Miller, C.F., and Barton, M.D., 1990, Phanerozoic plutonism in the Cordilleran interior, U.S.A.: Geological Society of America Special Paper 241, p. 213–232.

Miyashiro, A., 1974, Volcanic rock series in island arcs and active continental margins: American Journal of Science, v. 274, p. 321–355.

Monroe, S.C., Godlewski, D.W., and Plahuta, J.T., 1988, Geology and mineralization at the Buckhorn mine, Eureka County, Nevada, *in* Schafer, R.W., Cooper, J.J., and Vikre, P.G., eds., Bulk mineable precious metal deposits of the western United States. Symposium proceedings: Reno, Geological Society of Nevada, p. 273–291.

Morris, G.A., Larson, P.B., and Hooper, P.R., 2001, "Subduction style" magmatism in a non-subduction setting: the Colville Igneous Complex, NE Washington state, USA: Journal of Petrology, v. 41, p. 43–67.

Muntean, J., Tarnocai, C., Coward, M., Rouby, D., and Jackson, A., 2001, Styles and restorations of Tertiary extension in north-central Nevada: Reno, Geological Society of Nevada Special Publication 33, p. 55–69.

Nakamura, K., 1977, Volcanoes as possible indicators of tectonic stress orientation—principal and proposal: Journal of Volcanology and Geothermal Research, v. 2, p. 1–16.

Nash, J.T., and Trudel, W.S., 1996, Bulk mineable gold ore at the Sleeper mine, Nevada—importance of extensional faults, breccia, framboids, and oxidation: Geological Society of Nevada, Geology and Ore Deposits of the American Cordillera Symposium, Reno-Sparks, Nevada, April 1995, Proceedings, p. 235–256.

Nash, J.T., Utterback, W.C., and Saunders, J.A., 1991, Geology and geochemistry of the Sleeper gold deposits, Humboldt County, Nevada, an interim report, *in* Raines, G.L., Lisle, R.E., Schafer, R.W., and Wilkinson, W.H., eds., Geology and ore deposits of the Great Basin. Symposium proceedings: Reno, Geological Society of Nevada and U.S. Geological Survey, p. 1063–1084.

Nash, J.T., Utterback, W.C., and Trudel, W.C., 1995, Geology and geochemistry of Tertiary volcanic host rocks, Sleeper gold-silver deposit, Humboldt County, Nevada: U.S. Geological Survey Bulletin 2090, 63 p.

Noble, D. C., 1972, Some observations on the Cenozoic volcano-tectonic evolution of the Great Basin, western United States: Earth and Planetary Science Letters, v. 17, p. 142–150.

——1988, Cenozoic volcanic rocks of the northwestern Great Basin: An overview: Geological Society of Nevada Special Publication 7, p. 31–42.

Noble, D.C., McCormack, J.K., McKee, E.H., Silberman, M.L., and Wallace, A.B., 1988, Time of mineralization in the evolution of the McDermitt caldera complex, Nevada-Oregon, and the relation of middle Miocene mineralization in the northern Great Basin to coeval regional basaltic magmatic activity: ECONOMIC GEOLOGY, v. 83, p. 859–863.

Nolan, T.B., 1933, Epithermal precious-metal deposits of the western states (Lindgren volume): New York, American Institute of Mining and Metallurgical Engineers, p. 623–640.

——1935, Underground geology of the Tonopah mining district, Nevada: Nevada University Bulletin 29, no. 5.

Ohmoto, H., and Goldhaber, M.B., 1997, Sulfur and carbon isotopes, *in* Barnes, H. L., ed., Geochemistry of hydrothermal ore deposits, 3rd ed.: New York, John Wiley and Sons, p. 517–612.

Oldow, J.S., 1992, Late Cenozoic displacement partitioning in the northwestern Great Basin: Geological Society of Nevada, Structure, Tectonics and Mineralization of the Walker Lane Symposium, April 24, 1992, Reno, Proceedings, p. 17–52.

Oldow, J.S., Kohler, G., and Donelick, R.A., 1994, Late Cenozoic extensional transfer in the Walker Lane strike-slip belt, Nevada: Geology, v. 22, p. 637–640.

Oldow, J.S., Aiken, C.L.V., Hare, J.L., Ferguson, J.F., and Hardyman, R.F., 2001, Active displacement transfer and differential block motion within the central Walker Lane, western Great Basin: Geology, v. 29, p. 19–22.

O'Neil, J.R., and Silberman, M.L., 1974, Stable isotope relations in epithermal Au-Ag deposits: ECONOMIC GEOLOGY, v. 69, p. 902–909.

O'Neil, J.R., Silberman, M.L., Fabbi, B.P., and Chesterman, C.W., 1973, Stable isotope and chemical relations during mineralization in the Bodie mining district, Mono County, Nevada: ECONOMIC GEOLOGY, v. 68, p. 765–784.

Osborne, M.A., 1991, Epithermal mineralization at Aurora, Nevada, *in* Raines, G.L., Lisle, R.E., Schafer, R.W., and Wilkinson, W.H., eds., Geology and ore deposits of the Great Basin. Symposium proceedings: Reno, Geological Society of Nevada and U.S. Geological Survey, p. 1097–1110.

Parsons, T., Thompson, G.A., and Sleep, N.H., 1994, Mantle plume influence on the Neogene uplift and extension of the U.S. western Cordillera?: Geology, v. 22., p. 83–86.

Perkins, C., 1987, Geological and chemical comparison of two epithermal precious metal systems: The Late Permian Red Rock deposit, Drake Volcanics, New South Wales, Australia, and the Miocene Gooseberry deposit, Kate Peak Volcanics, Nevada: Unpublished Ph.D. dissertation, New South Wales, Australia, University of New England, 363 p.

Pierce, K.L., and Morgan, L.A., 1992, The track of the Yellowstone hot spot; volcanism, faulting, and uplift: Geological Society of America Memoir 179, p. 1–53.

Power, S., 1985, The "tops" of porphyry copper deposits, mineralization, and plutonism in the western Cascades, Oregon: Unpublished Ph.D. thesis, Corvallis, Oregon State University, 234 p.

Price, R.C., Stewart, R.B., Woodhead, J.D., and Smith, I.E.M., 1999, Petrogenesis of high-K arc magmas: Evidence from Egmont volcano, North Island, New Zealand: Journal of Petrology, v. 40, p. 167–197.

Proffett, J.M., Jr., 1977, Cenozoic geology of the Yerington district, Nevada, and implications for the nature and origin of Basin and Range faulting: Geological Society of America Bulletin, v. 88, p. 247–266.

Ransome, F.L., 1907, The association of alunite with gold in the Goldfield district, Nevada: ECONOMIC GEOLOGY, v. 2, p. 667–692.

Rye, R.O., Bethke, P.M., and Wasserman, M.D., 1992, The stable isotope geochemistry of acid-sulfate alteration: ECONOMIC GEOLOGY, v. 87, p. 225–262.

Rytuba, J.J., 1996, Cenozoic metallogeny of California: Geological Society of Nevada, Geology and Ore Deposits of the American Cordillera Symposium, Reno-Sparks, Nevada, April 1995, Proceedings, p. 803–822.

Rytuba, J.J., and Glanzman, R.K., 1979, Relation of mercury, uranium, and lithium deposits to McDermitt caldera complex, Nevada-Oregon: Nevada Bureau of Mines and Geology Report 33, p. 109–118.

Rytuba, J.J., and McKee, E.H., 1984, Peralkaline ash flow tuffs and calderas of the McDermitt volcanic field, southeast Oregon and north central Nevada: Journal of Geophysical Research, v. 89, p. 8616–8628.

Saunders, J.A., and Schoenly, P.A., 1995, Boiling, colloid nucleation and aggregation, and the genesis of bonanza Au-Ag ores of the Sleeper deposit, Nevada: Mineralium Deposita, v. 30, p. 199–210.

Saunders, J.A., Cook, R.B., and Schoenly, P.A., 1996, Electrum disequilibrium crystallization textures in volcanic-hosted bonanza epithermal gold deposits in northern Nevada: Geological Society of Nevada, Geology and Ore Deposits of the American Cordillera Symposium, Reno-Sparks, Nevada, April 1995, Proceedings, p. 173–179.

Seal, R.R., II, Essene, E.J., and Kelly, W.C., 1990, Tetrahedrite and tennantite: Evaluation of thermodynamic data and phase equilibria: Canadian Mineralogist, v. 28, p. 725–738.

Seedorff, E., 1991, Magmatism, extension, and ore deposits of Eocene to Holocene age in the Great Basin—mutual effects and preliminary proposed genetic relationships, *in* Raines, G.L., Lisle, R.E., Schafer, R.W., and Wilkinson, W.H., eds., Geology and ore deposits of the Great Basin. Symposium proceedings: Reno, Geological Society of Nevada and U.S. Geological Survey, p. 133–178.

Shinohara, H., and Hedenquist, J.W., 1997, Constraints on magma degassing beneath the Far Southeast porphyry Cu-Au deposit, Philippines: Journal of Petrology, v. 38, p. 1741–1752.

Silberman, M.L., Chesterman, C.W., Kleinhampl, F.J., and Gray, C.H., Jr., 1972, K-Ar ages of volcanic rocks and gold-bearing quartz-adularia veins in the Bodie mining district, Mono County, California: ECONOMIC GEOLOGY, v. 67, p. 597–603.

Silberman, M.L., Stewart, J.H., and McKee, E.H., 1976, Igneous activity, tectonics, and hydrothermal precious-metal deposits in the Great Basin during Cenozoic time: Society of Mining Engineers AIME Transactions, v. 260, p. 253–263.

Sillitoe, R.H., 2000, Gold-rich porphyry deposits: Descriptive and genetic models and their role in exploration and discovery: Reviews in Economic Geology, v. 13, p. 315–346.

Sillitoe, R.H., and Lorson, R.C., 1994, Epithermal gold-silver-mercury deposits at Paradise Peak, Nevada: Ore controls, porphyry gold association, detachment faulting, and supergene oxidation: ECONOMIC GEOLOGY, v. 89, p. 1228–1248.

Simmons, S.F., 1995, Magmatic contributions to low-sulfidation epithermal deposits: Mineralogical Association of Canada Short Course Series, v. 23, p. 455–477.

Simmons, S.F., and Browne, P.R.L., 2000, Hydrothermal minerals and precious metals in the Broadlands-Ohaaki geothermal system: Implications for understanding low-sulfidation epithermal environments: ECONOMIC GEOLOGY, v. 95, p. 971–999.

Simon, G., Kesler, S.E., and Essene, E.J., 1997, Phase relations among selenides, sulfides, tellurides, and oxides: II. Applications to selenide-bearing ore deposits: ECONOMIC GEOLOGY, v. 92, p. 468–484.

Snow, J.K., and Wernicke, B., 2000, Cenozoic tectonism in the central Basin and Range: Magnitude, rate, and distribution of upper crustal strain: American Journal of Science, v. 300, p. 659–719.

Sonder, L.J., and Jones, C.H., 1999, Western United States extension: How the west was widened: Annual Review of Earth and Planetary Sciences, v. 27, p. 417–462.

Stewart, J.H., 1980, Geology of Nevada: Nevada Bureau of Mines and Geology: Special Publication 4, 136 p.

——1988, Tectonics of the Walker Lane belt, western Great Basin: Mesozoic and Cenozoic deformation in a zone of shear, *in* Ernst, W. G., ed., The geotectonic development of California: Englewood Cliffs, New Jersey, Prentice-Hall, p. 71–86

Stewart, J.H., and Carlson, J.E., 1976, Cenozoic rocks of Nevada: Nevada Bureau of Mines and Geology Map 52, scale 1:1,000,000.

——1978, Geologic map of Nevada: Nevada Bureau of Mines and Geology, scale 1:500,000.

Takada, A., 1994, The influence of regional stress and magmatic input on styles of monogenetic and polygenetic volcanism: Journal of Geophysical Research, v. 99, p. 13,563–13,573.

Taylor, H.P., Jr., 1973, O^{18}/O^{16} evidence for meteoric-hydrothermal alteration and ore deposition in the Tonopah, Comstock Lode, and Goldfield mining districts, Nevada: ECONOMIC GEOLOGY, v. 68, p. 747–764.

Theodore, T.G., and Blake, D.W., 1978, Geology and geochemistry of the West orebody and associated skarns, Copper Canyon porphyry copper deposits, Lander County, Nevada: U.S. Geological Survey Professional Paper 798-C, 85 p.

Thompson, G.A., 1956, Geology of the Virginia City quadrangle, Nevada: U.S. Geological Survey Bulletin 1042-C, p. 45–77.

Thomson, K., Brummer, J.E., Caldwell, D.A., McLachlan, C.D., and Schumacher, A.L., 1993, Geology and geochemistry of the Mule Canyon gold deposit, Lander County, Nevada: Society for Mining, Metallurgy, and Exploration Preprint 93-271, 10 p.

Tosdal, R.M., and Richards, J.P., 2001, Magmatic and structural controls on the development of porphyry Cu ± Mo ± Au deposits: Reviews in Economic Geology, v. 14, p. 157–181.

Van Nieuwenhuyse, R., 1991, Geology and ore controls of gold-silver mineralization in the Talapoosa mining district, Lyon County, Nevada: Geological Society of Nevada, Geology and Ore Deposits of the Great Basin Symposium, April 1990, Reno, Nevada, Proceedings, p. 979–993.

Vikre, P.G., 1985, Precious metal vein systems in the National district, Humboldt County, Nevada: ECONOMIC GEOLOGY, v. 80, p. 360–393.

——1987, Paleohydrology of Buckskin Mountain, National district, Humboldt County, Nevada: ECONOMIC GEOLOGY, v. 82, p. 934–950.

——1989a, Fluid-mineral relations in the Comstock Lode: ECONOMIC GEOLOGY, v. 84, 1574–1613.

——1989b, Ledge formation at the Sandstorm and Kendell gold mines, Goldfield, Nevada: ECONOMIC GEOLOGY, v. 84, p. 2115–2138.

——1998, Quartz-alunite alteration in the western part of the Virginia Range, Washoe and Storey Counties, Nevada: ECONOMIC GEOLOGY, v. 93, p. 338–346.

——2000, Elemental sulfur (S°) deposits and S° associated with precious metals, mercury, and thermal springs in the Great Basin: Geological Society of Nevada, Geology and Ore Deposits 2000: The Great Basin and Beyond Symposium, May 15–18, 2000, Reno-Sparks, Nevada, Proceedings, p. 735–767.

Vikre, P.G., McKee, E.H., and Silberman, M.L., 1988, Chronology of Miocene hydrothermal and igneous events in the western Virginia Range, Washoe, Storey, and Lyon Counties, Nevada: ECONOMIC GEOLOGY, v. 83, p. 864–874.

Vogel, T.A., Cambray, F.W., Feher, L., Constenius, K.N., and the WIB Research Group, 1998, Petrochemistry and emplacement history of the Wasatch igneous: Society of Economic Geologists Guidebook 29, 2nd ed., p. 35–46.

Vogel, T.A., Cambray, F.W., and Constenius, K.N., 2001, Chemical variation in the Wasatch igneous belt, central Wasatch Mountains, Utah: Evidence for a non-subduction origin: Rocky Mountain Geology (in press).

Wallace, A.B., 1979, Possible signatures of buried porphyry-copper deposits in middle to late Tertiary volcanic rocks of western Nevada: Nevada Bureau of Mines and Geology Report 33, p. 69–76.

Wallace, A.R., 1993, Geologic map of the Snowstorm Mountains and vicinity, Elko and Humboldt Counties, Nevada: U.S. Geological Survey Miscellaneous Investigations Map I-2394, scale 1:50,000.

Wallace, A.R., and John, D.A., 1998, New studies of Tertiary volcanic rocks and mineral deposits, northern Nevada rift: U.S. Geological Survey Open-File Report 98-338, p. 264–278.

Wernicke, B.P., 1985, Uniform-sense normal simple shear of the continental lithosphere: Canadian Journal of Earth Sciences, v. 22, p. 108–125.

——1992, Cenozoic extensional tectonics of the U.S. Cordillera: Geological Society of America, Geology of North America, v. G-3, p. 553–581.

Wernicke, B.P., Christiansen, R.L., England, P.C., and Sonder, L.J., 1987, Tectonomagmatic evolution of Cenozoic extension of the North American Cordillera: Geological Society of London Special Publication 28, p. 203–222.

Westra, G., and Riedell, K.B., 1996, Geology of the Mount Hope stockwork molybdenum deposit, Eureka County, Nevada: Geological Society of Nevada, Geology and Ore Deposits of the American Cordillera Symposium, Reno-Sparks, Nevada, April 1995, Proceedings, p. 1639–1666.

White, D.E., 1955, Thermal springs and epithermal ore deposits: ECONOMIC GEOLOGY 50TH ANNIVERSARY VOLUME, p. 99–154.

——1981, Active geothermal systems and hydrothermal ore deposits: ECONOMIC GEOLOGY 75TH ANNIVERSARY VOLUME, p. 392–423.

White, N.C., and Hedenquist, J.W., 1990, Epithermal environments and styles of mineralization: Variations and their causes, and guidelines for exploration: Journal of Geochemical Exploration, v. 36, p. 445–474.

Whitebread, D.H., 1976, Alteration and geochemistry of Tertiary volcanic rocks in parts of the Virginia City quadrangle, Nevada: U.S. Geological Survey Professional Paper 936, 43 p.

Whitney, J.A., 1984, Fugacities of sulfurous gases in pyrrhotite-bearing silicic magmas: American Mineralogist, v. 69, p. 69–78.

——1988, Composition and activity of sulfurous species in quenched magmatic gases associated with pyrrhotite-bearing silicic systems: ECONOMIC GEOLOGY, v. 83, p. 86–92.

Wilshire, H.G., 1957, Propylitization of Tertiary volcanic rocks near Ebbetts Pass, Alpine County, California: University of California Publications in Geological Sciences, v. 32, p. 243–272.

Wood, J.D., 1991, Geology of the Wind Mountain gold deposit, Washoe County, Nevada: Geological Society of Nevada, Geology and Ore Deposits of the Great Basin Symposium, April 1990, Reno, Nevada, Proceedings, p. 1051–1061.

Zoback, M.L., and Thompson, G.A., 1978, Basin and Range rifting in northern Nevada: Clues from a mid-Miocene rift and its subsequent offsets: Geology, v. 6, p. 111–116.

Zoback, M.L., Anderson, R.E., and Thompson, G.A., 1981, Cainozoic evolution of the state of stress and style of tectonism of the Basin and Range province: Philosophical Transactions of the Royal Society of London, v. A300, p. 407–434.

Zoback, M.L., McKee, E.H., Blakely, R.J., and Thompson, G.A., 1994, The northern Nevada rift: Regional tectonomagmatic relations and middle Miocene stress direction: Geological Society of America Bulletin, v. 106, p. 371–382.